VOL. 9 No. 11, pp. 321-348 1947/1948

Philips Technical Review

DEALING WITH TECHNICAL PROBLEMS
RELATING TO THE PRODUCTS, PROCESSES AND INVESTIGATIONS OF
THE PHILIPS INDUSTRIES

EDITED BY THE RESEARCH LABORATORY OF N.V. PHILIPS' GLOEILAMPENFABRIEKEN, EINDHOVEN, NETHERLANDS.

THE LIGHT-EMISSION OF X-RAY SCREENS

by H. A. KLASENS *) and W. de GROOT.

537.531:535.371

This article reviews the various ways in which fluorescent screens are employed in radiography and discusses the factors determining the brightness of a viewing screen or the darkening of a photographic image obtained with the aid of an intensifying screen. The factors referred to are:

1) the absorption of X-rays in the screen;
2) the conversion of absorbed X-ray energy into energy of fast electrons formed in the mass of the screen;
3) the conversion of the electron energy into light energy or photographically active radiation;
4) the absorption and the scattering of light in the screen;
5) the selectivity of the eye or of the photographic emulsion relative to the spectral distribution of the radiated fluorescent light.

The optimum thickness for viewing and intensifying screens and the most suitable luminophores are investigated. It is shown that for intensifying purposes, when using low tube voltages (less than 70 kV), ZnS screens are to be preferred to $CaWO_4$ screens.

Introduction

Fluorescent screens play an important part in radiography. In the first place they are used as viewing screens for diagnostical purposes and for the examination of materials. In the second place a fluorescent screen is needed in screen photography, when the image formed on the screen is photographed by a camera. In the third place fluorescent screens are used as intensifying screens for producing a direct image on a photographic film, where the fluorescing layer is in immediate contact with the sensitized material.

In all cases the fluorescent screen consists of a layer of very small crystals of substances such as zinc sulphide (ZnS) or calcium tungstate ($CaWO_4$), which have the property of converting the absorbed X-ray energy into visible or photographically active rays. These crystals are held together by a binder, usually an organic substance, which cements the crystals together in a smooth layer. This layer of crystals with binder is applied on a thin base of white cardboard to give it the necessary firmness. Cardboard is chosen because in many cases it is necessary that the base should not obstruct the passage of the X-rays; it will be seen farther on why the cardboard must be white.

Fig. 1 illustrates diagrammatically the use of a fluorescent screen as a viewing screen or in screen photography. The X-rays coming from the left, possibly reduced in strength by the object *A*, strike the cardboard base (*1*) of the screen *S* and pass through it into the fluorescent layer (*2*). Owing to the differences in transmission between the parts of the object there are differences of brightness in the fluorescent layer, so that a "shadow image" of the

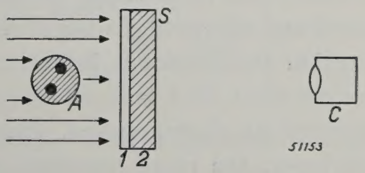

Fig. 1. Diagrammatic representation of the arrangement of a viewing screen or an arrangement for screen-image photography. *A* = object, *C* = the eye or camera, *1* = cardboard base, *2* = fluorescent layer.

---

*) Material Research Laboratory, Philips Electrical Ltd., London, England.

object can be observed in all its details. C is the eye or the camera.

Fig. 2 illustrates the various ways in which an intensifying screen can be used. In fig. 2*a* we see a front screen with the cardboard side facing the X-ray tube as in fig. 1. The photographically active layer (*3*) applied on a celluloid film (*4*) is in immediate contact with the fluorescent layer (*2*).

Fig. 2*b* shows a fluorescent screen used as a back screen, where the X-rays first pass through the celluoid (*4*) and the sensitized layer (*3*) of the film and then through the immediately adjacent fluorescent layer (*2*). Fig. 2*c* shows a frequently applied combination of a front screen and a back screen: the film is usually covered with a sensitized layer on both sides (*3*) and (*5*), against which fluorescent layers (*2*) and (*6*) of the screens are laid.

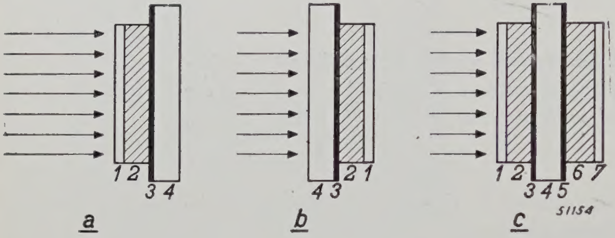

Fig. 2. Diagram showing how intensifying screens are used. *a*) front screen, *b*) back screen, *c*) front and back screens. *1* and *7* cardboard base, *2* and *6* fluorescent layer, *3* and *5* sensitized layer, *4* celluloid.

The X-rays absorbed in the fluorescent layer release electrons which cause that layer to glow. Primarily the luminous intensity of the image is therefore proportional to the amount of X-ray energy absorbed. But not all the light coming from the crystals of the fluorescent substance emerges from the fluorescent layer itself, because a part of it is scattered and absorbed. Owing to this scattering and absorption the luminous intensity is reduced and moreover there is a lack of sharpness in the image observed or photographed. The thicker the fluorescent layer, the more pronounced these two effects become. When the screen is used as an intensifying screen then the sensitized layer of the film is also struck directly by the X-rays, but these only contribute towards the darkening to a small extent (3 to 10%), mainly because the X-rays used in radiography are only to a small extent absorbed in the photographic emulsion layers. The visible or ultra-violet light generated in the fluorescent layer thereby causes an intensification (shortening of the exposure time) by a factor of 10 to 30.

This factor would be considerably smaller if a larger fraction of the X-ray energy could be absorbed in the photographic emulsion itself, for instance by making it much thicker. This, however, is not very feasible, for practical reasons. In crystal structure analysis X-rays of much longer wavelength than those used in Röntgenology are used. These rays are much more strongly absorbed in the normal photographic emulsion and consequently the use of intensifying screens is of little advantage in this case.

With a given intensity of X-rays it is obviously of importance to obtain the highest possible luminous intensity or actinic action of the screen. The object of this article is to investigate the factors influencing the brightness of the screen.

The absorbed X-ray energy

We may imagine X-rays as being a rain of quanta, each having an energy $h\nu$ (ν = frequency, h = Planck's constant = 6.62×10^{-34} watt sec^2).

Upon striking a substance these X-rays are attenuated in two ways, firstly by absorption, the energy $h\nu$ of the quantum (less the ionization energy) being transmitted to an electron which is thereby released from the atom struck, and secondly by scattering, the rays being only changed in direction without loss of energy. Since, however, with the substances from which fluorescent screens are made the tendency of X-rays to be scattered is small compared with the absorption, this scattering will be left out of consideration.

The consequence of scattering is that the average path travelled by a quantum in the layer is somewhat greater than the thickness D of the screen, and as a result there is a slight increase in the total absorption.

For a screen consisting of a certain kind of atoms the number of quanta absorbed per second per square centimeter in a layer of a thickness dx will be:

$$N_0\, n\, a\, \mathrm{d}x,$$

in which N_0 represents the number of incident quanta per cm^2, n the number of atoms per cm^3 and a the cross section for absorption per atom.

$$\text{Since } n = \frac{\text{mass per cm}^3}{\text{mass per atom}} = \frac{\varrho}{A/N_A}$$

(ϱ = density in g/cm^3, A = atomic weight, N_A = 6.023×10^{23} = the Avogadro number),

$$N_0\, n\, a\, \mathrm{d}x = N_0 \frac{\varrho a N_A}{A} \mathrm{d}x = N_0 \mu \mathrm{d}x, \quad . \ . \quad (1)$$

where $\mu = \varrho a N_A / A$ is the so-called absorption coefficient.

In the case of a compound consisting of more than one kind of atom

$$a_{mol} = n_1a_1 + n_2a_2 + \ldots ,$$

where n_1, n_2, ... represent the number of atoms per molecule, whilst

$$\mu = \frac{\varrho a_{mol} N_A}{M},$$

where ϱ represents the density of the compound and

$$M = n_1A_1 + n_2A_2 + \ldots$$

is the molecular weight of the compound.

The quantity a, as we have seen, is related to the release of an electron from the atom. It depends upon the frequency ν, and thus also upon the wavelength $\lambda = c/\nu$ (c = velocity of light), such that

$$a = C{\cdot}Z^4{\cdot}\lambda^3 . \quad . \quad . \quad . \quad . \quad . \quad . \quad . \qquad (2)$$

in which Z is the atomic number of the element absorbing the X-rays. As the wavelength is shortened (frequency raised) a decreases until a frequency is reached at which a more tightly bound electron can be released. The constant C then suddenly jumps to a higher value, and the frequency or the wavelength at which this jump takes place is called the absorption limit or absorption edge (*fig. 3*).

On the so-called K-edge, corresponding to the release of a K-electron (an electron bound in the innermost "shell" of an atom), with which we are most concerned in our case, C (λ in Å) jumps from the value

$$0.3{\cdot}10^{-26} \text{ for } \lambda_K < \lambda < \lambda_L\,^{1)}$$

to

$$2.3{\cdot}10^{-26} \text{ for } \lambda < \lambda_K .$$

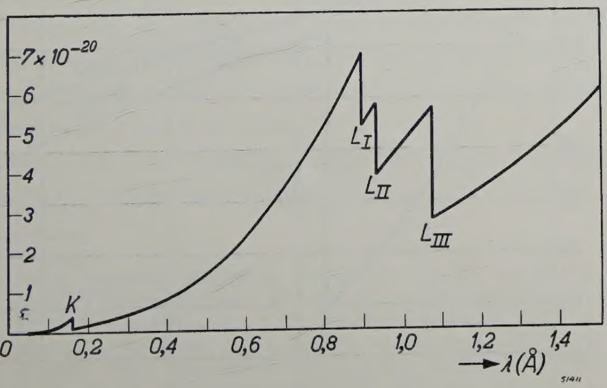

Fig. 3. Graph representing the absorption a as function of the wavelength λ for the element Pb. The single K-absorption edge and the three-fold L-absorption edge occur when the quantum of X-rays is large enough to release an electron from the K and the L shells respectively.

Fig. 4 gives the absorption coefficients of the compounds $CaWO_4$ and ZnS. The absorption edge (K-edge) in the curve for $CaWO_4$ is due to the W-atoms. The absorption edges of Ca, O, Zn and S and the L-edge of W fall outside the graph.

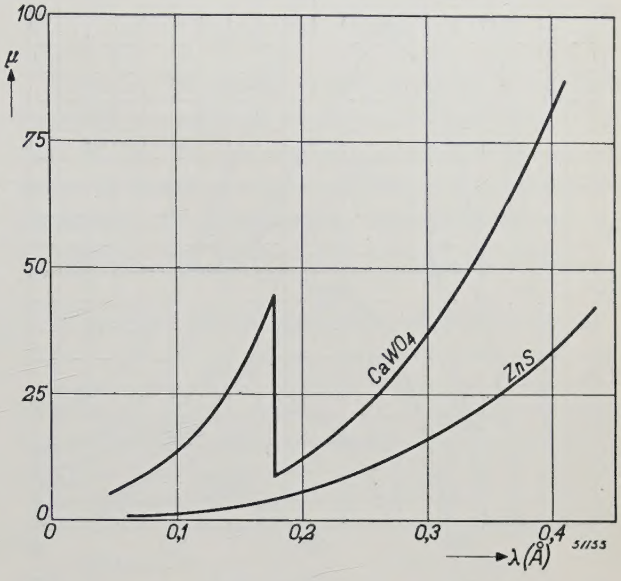

Fig. 4. Graphical representation of the absorption coefficient μ (in cm^{-1}) as function of the wavelength λ (in Ångström) for $CaWO_4$ and ZnS.

Taking "monochromatic" X-rays, the number of quanta passing through a finite layer of the thickness D is $N_0e^{-\mu D}$ and the energy absorbed is:

$$N_0h\nu\ (1-e^{-\mu D}) \quad . \quad . \quad . \quad . \quad . \quad . \qquad (3)$$

In practice we never have monochromatic X-rays, and this makes the calculation more complicated. The distribution of the continuous X-ray energy (the characteristic radiation does not play an important part here) among the various wavelengths is represented by the curves in *fig. 5*. The shortest wavelength in the continuous X-ray spectrum is given by the equation

$$\lambda_{\text{min}} = \frac{12.4}{V}, \quad . \quad . \quad . \quad . \quad . \quad . \qquad (4a)$$

the wavelength λ being expressed in Ångström and the tube voltage V in kV. When, as is usual, the rays are filtered through a thin metal plate, the long-wave rays are suppressed, the maximum intensity then being about $\lambda = 20/V$. The calculation can be simplified by assuming the radiation to be monochromatic with a wavelength

$$\lambda_{\text{eff}} = \frac{20}{V} . \quad . \quad . \quad . \quad . \quad . \quad . \quad . \qquad (4b)$$

With a tube voltage of 50 kV, thus with λ_{eff} = 0.4 Å, the value of μ in a ZnS screen is 30 cm^{-1} and

---

1) For the sake of simplicity the three-fold absorption edge is regarded as a simple edge.

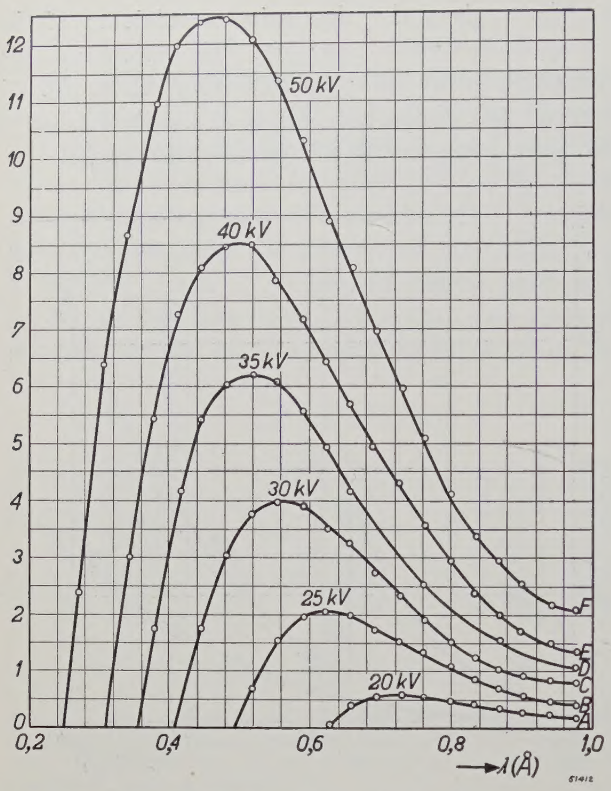

Fig. 5. Energy distribution in the continuous X-ray spectrum as a function of the wavelength λ for various voltages between 20 and 50 kV. With increasing tube voltage the peak of the graph is shifted to the left and the value of λ_{min}, the shortest wavelength in the radiation, becomes smaller. The intensity is given on the vertical axis on an arbitrary scale.

in a $CaWO_4$ screen 80 cm^{-1}. In a layer of zinc sulphide 0.03 cm thick, which is reasonable for a fluorescent screen, about 60% of the X-ray energy is then absorbed.

The conversion of X-ray energy into light energy

As we have seen, the X-ray energy is converted into light energy in two stages:

1) conversion of the absorbed quantum of X-rays into a rapid electron;
2) conversion of the energy of the electron into the energy of the fluorescent radiation.

From one energy unit of absorbed X-rays k energy units of light radiation are obtained ($k < 1$), for which we write:

$$k = k_{re} \cdot k_{el} \quad . \; . \; . \; . \; . \; . \; . \quad (5)$$

in which k_{re} relates to the process 1) and k_{el} to 2). We shall now consider these two coefficients k_{re} and k_{el} separately.

The conversion of X-ray energy into electron energy

The quantity k_{re} is easily calculated. Assuming that a K-electron is released from the atom, the energy expended is $h\nu_K$, in which ν_K is the frequency of the K-edge. The energy imparted to the electron is then $h\nu—h\nu_K$, so that in this case the yield is

$$\frac{\text{electron energy}}{\text{X-ray energy}} = \frac{\nu - \nu_K}{\nu} = k_K .$$

Similarly, for the release of an L-electron we have:

$$\frac{\nu - \nu_L}{\nu} = k_L .$$

Since ν_L is usually very much smaller than ν, this last fraction may be taken as being equal to 1, whilst if $\nu > \nu_K$ the chance of L-absorption may be ignored. Hence per atom one may write:

$$k_{re} = \frac{\nu - \nu_K}{\nu} \quad (\nu > \nu_K, \lambda < \lambda_K) \quad . \quad (6a)$$

$$k_{re} = 1 \quad (\nu < \nu_K, \lambda > \lambda_K) \quad . \; . \; . \quad (6b)$$

By determining the average of these coefficients for all kinds of atoms we find the value of k_{re} for the whole screen.

In *fig. 6* k_{re} is plotted as a function of the wavelength for two screen substances ($CaWO_4$ and ZnS).

When a K-electron is ejected from the atom then an L-electron may fall into the unoccupied K-orbit, with the emission of a quantum whose frequency is less than $\nu < \nu_K$ (X-ray-fluorescent radiation or characteristic radiation). If this quantum is absorbed in the layer it cannot release another K-electron but can release an L-electron. We shall disregard this process, although actually k_{re} is thereby increased a little and, if the frequency is greater than ν_K, approaches more closely to the value 1.

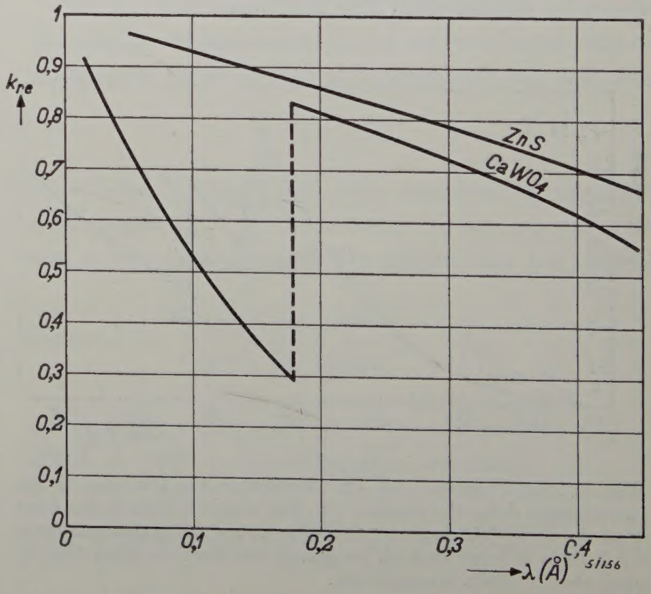

Fig. 6. The yield k_{re} from the conversion of X-rays into electron energy as function of the wavelength λ for $CaWO_4$ and ZnS.

Conversion of electron energy into light

As to the conversion characterized by k_{el}, much is already known from measurements of the light yield of cathode-ray tubes. In these tubes a fluorescent screen is struck directly by fast electrons. It has been found that in the case of electrons having an energy of 50 kV and more the light energy generated may amount to 10% of the electron energy.

Further, k_{el} can of course be deduced from measurements of the luminous intensity of a fluorescent screen irradiated with X-rays or with gamma rays [2]). From these measurements, too, it is to be deduced that

$$k_{el} = 0.05 - 0.1.$$

Scattering and absorption of light in the screen

Let us assume that we have a screen of the thickness D which is homogeneously irradiated with X-rays, and confine our attention to one particular crystal at a distance x below the surface which is brought to luminosity by the radiation. On its way to the free side of the screen the light from this crystal will be scattered (but without loss of energy) and subsequently absorbed (energy being thereby lost). Consequently the available light energy will be less than

$$k \cdot N_0 h\nu \; (1 - e^{-\mu D}).$$

Extensive calculations concerning the influence of absorption and scattering have been made by Hamaker [3]), who also took into consideration the reflection of the light from the cardboard layer and, where present, the photographic film. It if were not reflected by the cardboard then a considerable portion of the light energy would be lost on the "wrong" side of the fluorescent layer, and that is why white cardboard is used as base.

Hamaker's formulae for the light energy emitted per cm² are as follows:

$$J_B = A \cdot kN_0 h\nu \, \frac{\mu}{\mu + \sigma} \, (1 - e^{-(\mu+\sigma)D}) \quad . \; . \; . \; . \; . \quad (7)$$

$$J_F = A \cdot kN_0 h\nu \, \frac{\mu}{\mu - \sigma} \, (e^{-\sigma D} - e^{-\mu D}) \quad . \; . \; . \; . \; . \quad (8)$$

$$J_S = B \cdot kN_0 h\nu \, \frac{\mu}{\mu - \sigma} \, (e^{-\sigma D} - e^{-\mu D}) \quad . \; . \; . \; . \; . \quad (9)$$

Equation (9) applies to the case of fig. 1 (viewing screens), equation (8) to that of fig. 2*a*, and (7) to that of fig. 2*b* (intensifying screens). The coefficients A and B are generally 0.5 to 1, whilst σ is a coefficient of attenuation, related both to the absorption and to the scattering of the light.

The equation for the attenuation coefficient σ is:

$$\sigma = \sqrt{\mu_l\,(\mu_l + 2\sigma_l)} \quad . \; . \; . \; . \; . \; . \; . \quad (10)$$

in which μ_l represents the absorption coefficient (in diffuse light) and σ_l the scattering coefficient of the layer, both for light.

The coefficients A and B are equal to

$$A = \frac{1 + \varrho_1}{2\,(\varrho_1 + \beta)}, \qquad B = \frac{1}{1 + \beta},$$

where $\varrho_1 = (1 - r_1)/(1 + r_1)$, in which r_1 represents the reflectivity of the film, whilst $\beta = (1 - R_\infty)/(1 + R_\infty)$, R_∞ indicating the reflection coefficient of an infinitely thick fluorescent layer. In the derivation of equations (7) to (9) it has been assumed that $\beta = \varrho_2 = (1 - r_2)/(1 + r_2)$, where r_2 represents the reflection coefficient of the cardboard. If this condition does not exist then the equations become much more complicated [3]). This assumption, however, is by no means imaginary, for it appears that both β and ϱ_2 are very much less than 1, or r_2 and R_∞ are approximately equal to 1. Further, absorption of the X-rays in the cardboard is ignored.

Hamaker's formulae show a great similarity to the formulae previously deduced by Glocker and his fellow-workers [4]), viz:

$$J_B = kN_0 h\nu \, \frac{\mu}{\mu + \tau} \, (1 - e^{-(\mu+\tau)D}) \quad . \; . \; . \quad (11)$$

$$J_F = kN_0 h\nu \, \frac{\mu}{\mu - \tau} \, (e^{-\tau D} - e^{-\mu D}) \quad . \; . \; . \; . \quad (12)$$

These formulae have the advantage that they can easily be deduced by integration, by assuming that a fraction $e^{-\tau x}$ or $e^{-\tau(D-x)}$ of a quantity of light generated at a depth x in the fluorescent layer emerges at the surface (here the layer is assumed to be without a cardboard base), so that

$$J_B = kN_0 h\nu \int_0^D \mu e^{-\mu x} \cdot e^{-\tau x}\, dx,$$

$$J_F = kN_0 h\nu \int_0^D \mu e^{-\mu x} \cdot e^{-\tau(D+x)}\, dx.$$

Here τ has the character of a pure absorption in contrast to σ, which quantity depends upon absorption and scattering.

The quantity σ can be determined experimentally by measuring the quantity J_B/J_F, which depends only upon μ and σ; if the chemical composition of the screen is known, μ can be calculated in the manner indicated above.

---

[2]) In a recently published article by J. W. Coltman, E. G. Ebbinghausen and N. Altar (J. Appl. Physics **18**, 530-544, 1947, No. 6) it has been deduced from the luminous intensity of a CaWO$_4$ screen irradiated with X-rays that the value of k_{el} for CaWO$_4$ is 0.05. J. H. Born, N. Riehl and K. G. Zimmer. (Reichsber. Phys. **1**, 154-158, 1945) give for ZnS-Cu a much higher value, viz: $k_{el} = 0.71$, but the value given by Riehl himself for the conversion of alpha rays into light, viz: $k_{al} = 0.80$, is much higher than the values quoted by other authors (see H. A. Klasens, Trans. Faraday Soc. **42**, 666-668, No. 11). When the corrections indicated by Klasens are applied to the calculation one finds from the same experimental data for ZnS $k_{el} = 0.05$ to 0.1.

[3]) H. C. Hamaker, Philips Res. Rep. **2**, 55-67, 1947 (No.1).

[4]) R. Glocker, E. Kaupp, H. Widmann, Ann. phys. Leipzig, **85**, 313-332, 1928.

It appears that σ decreases with increasing crystal size. With different X-ray screens its value varies rather considerably, being of the order of 10 to 100 cm^{-1}.

Light intensity as a function of D

From equations (7) to (9) three conclusions can be drawn:

1) From (7) it appears that when a fluorescent screen is used as a back screen the amount of light energy radiated per cm^2 approaches a limiting value with increasing thickness of the screen, this being equal to 0.99 of the maximum light energy available when the thickness $D = 4.6/(\mu + \sigma)$; for $\mu = \sigma = 50$ this thickness is 0.046 cm.

2) When the fluorescent screen is used as a front screen or as a viewing screen it is possible to find the value of D at which the light energy is a maximum by differentiating formula (8) or (9) with respect to D:

$$\frac{\mathrm{d}J}{\mathrm{d}D} \sim \frac{\mu e^{-\mu D} - \sigma e^{-\sigma D}}{\mu - \sigma} \quad . \; . \; . \; . \; . \quad (13)$$

Taking this differential quotient as being equal to zero, it follows that:

$$D_{\text{opt}} = \frac{\ln(\sigma/\mu)}{\sigma - \mu} \quad . \; . \; . \; . \; . \quad (14)$$

In *fig. 7* D_{opt} is plotted as a function of μ for some values of σ.

By substituting the value of D_{opt} in (9) for instance we get

$$(J_S)_{\max} = B \cdot kN_0 h\nu \cdot F\left(\frac{\sigma}{\mu}\right) \quad . \; . \quad (15)$$

in which

$$F\left(\frac{\sigma}{\mu}\right) = \left(\frac{\sigma}{\mu}\right)^{\frac{\sigma}{\mu-\sigma}} \quad . \; . \; . \; . \; . \quad (16)$$

This quantity is represented in *fig. 8* as a function of σ/μ.

3) The case of a combined front and back screen is somewhat more complicated. First of all it must be said that the use of a film sensitized on both sides and with two adjacent screens offers great advantages over a film sensitized on one side used with one screen. In the first place, given the same quantity of light energy, the photographic density is more intense.

This is due to the fact that with increasing light energy L the density z increases less than proportionately with L, as is represented, for instance, by the empirical formula

$$z = E \log(1 + pL), \quad . \; . \; . \; . \; . \; . \quad (17)$$

in which E and p are constants. From *fig. 9*, in which z is plotted as a function of L, it appears that

$$z(L_1) + z(L_2) > z(L),$$

when

$$L_1 + L_2 = L.$$

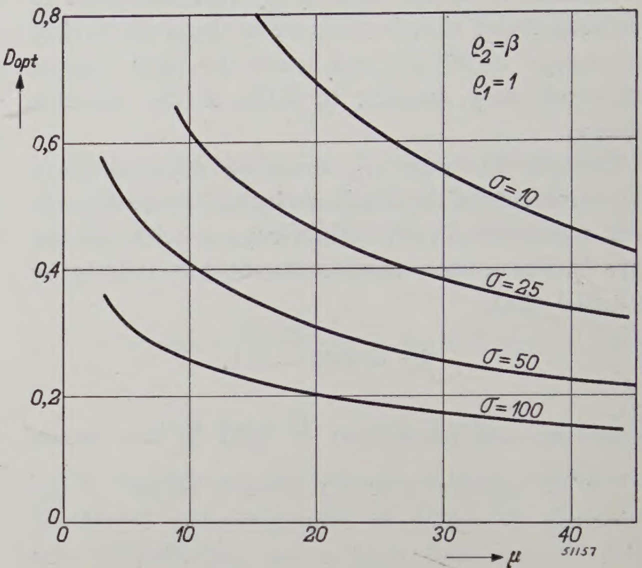

Fig. 7. The optimum thickness (in mm) of a viewing screen as function of the absorption coefficient μ for several values of the attenuation coefficient σ. Here it is assumed that $\varrho_2 = (1-r_2)/(1+r_2)$ (in which r_2 = the reflectivity coefficient of the cardboard) is equal to $\beta = (1-R_\infty)/(1+R_\infty)$ (in which R_∞ = the reflectivity coefficient of an infinitely thick fluorescent layer) and that r_1, the reflectivity of the film for light, is so small that $\varrho_1 = (1-r_1)/(1+r_1)$ can be taken as equal to 1.

This can also be easily demonstrated analytically. At the same time it appears that

$z(L_1) + z(L_2)$ has a maximum when $L_1 = L_2 = L/2$.

The second advantage in using more than one screen lies in the fact that with two thin screens placed one behind the other more light is obtained than from one screen of the same thickness as that of the two thin ones together. In both cases, it is true, the same amount of X-ray energy is absorbed, but when two thin screens are used more

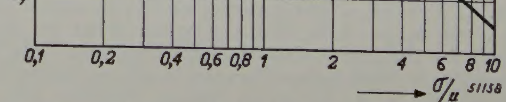

Fig. 8. The quantities $F(\sigma/\mu) = (\sigma/\mu)^{\sigma/(\mu-\sigma)}$ and $G(\sigma/\mu) = (^1/_2 + \sigma/2\mu)^{\sigma/(\mu-\sigma)}$ as functions of σ/μ, where σ represents the attenuation, are used for determining the optimum thickness of viewing screens and of front screens respectively.

light energy is released, because there is less absorption of light.

Theoretically one might therefore expect a maximum photographic effect when a large number of films are used, each being separated from the next by a thin screen. The light rays would then have to pass through no more than the thickness of a thin intermediate screen before acting upon a film. If, on the other hand, one thick screen, is used the light has to pass through deep layers where it is strongly absorbed before emerging. An improvement is obtained when we use a thick fluorescent layer as back screen and a thin foil as front screen as is done in practice. The truth of this argument has been experimentrlly confirmed by Barth and Eggert[5]) from an investigation with a combination of two films and four screens.

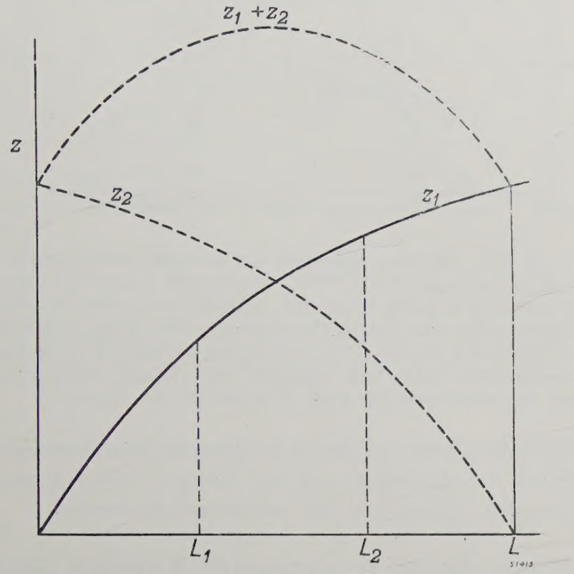

Fig. 9. Graphical representation of the blackening z as function of the light energy L according to formula (17). It is seen that $z(L_1) + z(L_2) > z(L)$ for $L_1 + L_2 = L$. The left-hand member of this inequality reaches its maximum for $L_1 = L_2 = L/2$.

In the same way as has been done for viewing screens and for simple front screens, we can now investigate what the optimum thickness of a front screen is when this is used in combination with the back screen.

If the back screen is taken to be of "infinite thickness" then the available energy is

$$J_B + J_F = A \cdot kN_0 h\nu \mu \left(\frac{e^{-\mu D}}{\mu + \sigma} + \frac{e^{-\sigma D} - e^{-\mu D}}{\mu - \sigma}\right). \quad (18)$$

Differentiation with respect to D yields:

$$D_{\text{opt}} = \frac{\ln\,[2\mu/(\mu+\sigma)]}{\mu - \sigma} \quad . \; . \; . \; . \quad (19)$$

In *fig. 10* D_{opt} is plotted as a function of μ for several values of σ. When we compare fig. 10 with fig. 7 it is found that with equal values of σ and μ and an infinitely thick back screen the optimum thickness of a front screen is smaller than that of a scanning screen.

By substitution in (18) we obtain:

$$(J_B + J_F)_{\max} = A \cdot kN_0 h\nu \cdot G\left(\frac{\sigma}{\mu}\right), \; . \; . \quad (20)$$

in which

$$G\left(\frac{\sigma}{\mu}\right) = \left(\frac{\mu + \sigma}{2\mu}\right)^{\frac{\sigma}{\mu - \sigma}} \quad . \; . \; . \; . \; . \quad (21)$$

This quantity is also shown in fig. 8 as a function of σ/μ.

Further, it appears that when the maximum effect is reached[6])

$$(J_B)_{\text{opt}} = (J_F)_{\text{opt}}.$$

The thinner the back screen is made, the larger is the optimum thickness of the front screen, until finally, when there is no back screen at all, it becomes equal to the optimum thickness of a viewing screen.

The utilisation of light energy by the eye or by the photographic emulsion

From the foregoing it can be deduced what factors have to be taken into account in order to

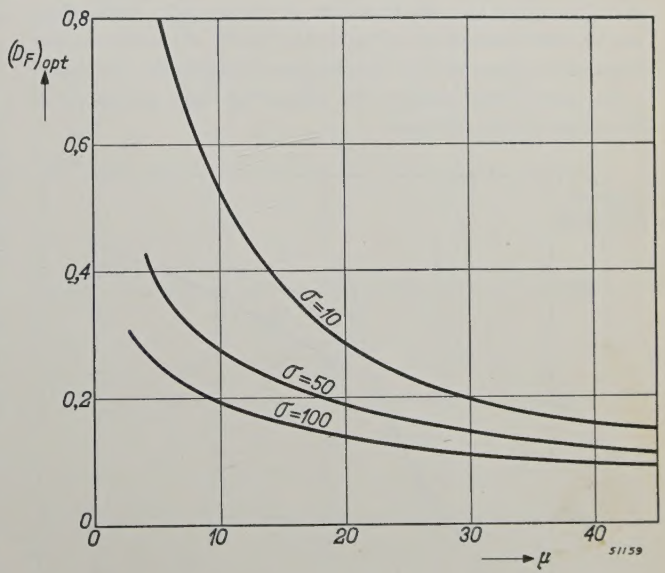

Fig. 10. The optimum thickness of the front screen (in mm) as function of the absorption coefficient μ for three values of the attenuation coefficient σ. Here it is assumed that the back screen is of infinite thickness.

---

[5]) W. Barth and J. Eggert, Fortschr. Rö. 39, 88-100, 1929.

[6]) It is interesting to note that this result agrees with the condition for a maximum photographic effect (the splitting up of a given quantity of light into two equal parts).

get a maximum amount of energy in the form of visible or photographically active light. The light stimulus brought about by this energy in our eye, or the darkening of the sentitized layer, depends, however, to a certain extent also upon the selective properties of the eye, or of the sensitized layer respectively, and the spectral composition of the fluorescent light.

With a high brightness (> 1 milli-Lambert) the maximum sensitivity of the eye lies at 5500 Å and with lower brightnesses (10^{-2}—10^{-5} milli-Lambert) such as occur with viewing screens it drops gradually to 5200 Å (Purkinje effect). For viewing screens one must therefore use substances whose maximum light emission lies around this wavelength.

Formely these screens used to be covered with barium platinocyanide (it was with the help of this substance that Röntgen discovered his X-rays) or with willemite ($ZnSiO_4$-Mn_2SiO_4), but these substances have a relatively low light yield. More suitable are substances such as ZnS-Cu or (60% Zn 40% Cd) S-Ag, which possess a high light yield. Moreover, this latter substance has a high μ value. From fig. 8 (curve F) it may be seen that given an equal value of σ (e.g. $\sigma = 50$) about twice as much light is obtained with a ZnCdS-screen ($\mu = 22$ for $\lambda = 0.25$ Å, V = 80 kV) as with a ZnS-screen ($\mu = 10$).

Sulphide screens are subject to slight decomposition when exposed to daylight, the resultant blackening being due to the ultra-violet and the blue rays of the sunlight. This effect can be counteracted by adding to the binder of the fluorescent substance a dyestuff (e.g. auramine) which absorbs the shortwave part of the sunlight but allows the light generated in the screen to pass through.

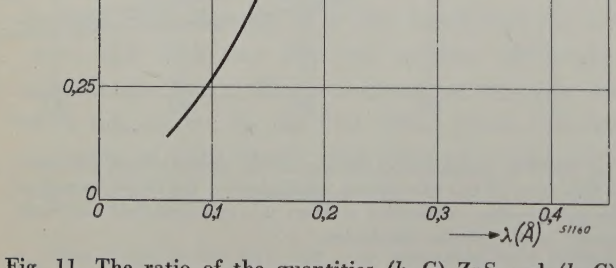

Fig. 11. The ratio of the quantities $(k_{re}G)$ ZnS and $(k_{re}G)$ $CaWO_4$ (for $\sigma = 50$) as function of the wavelength λ. Here k_{re} represents the efficiency of the transition from X-rays into electron energy, whilst G is the function illustrated in fig. 8.

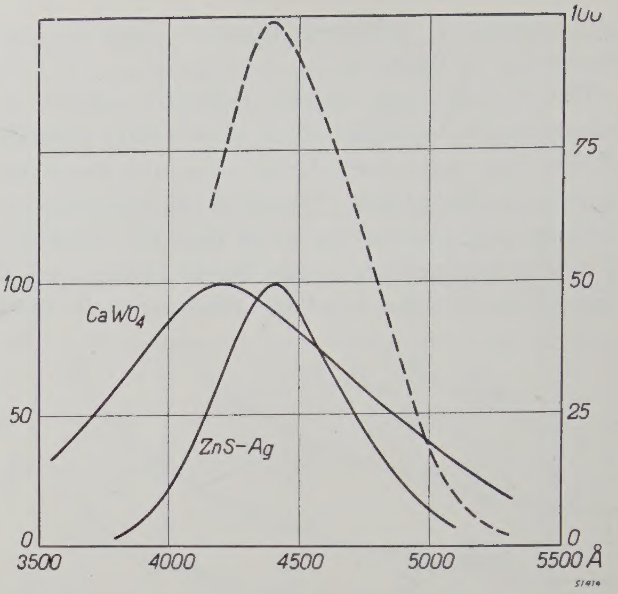

Fig. 12. The full lines represent the spectral distributions of the light emitted by a $CaWO_4$ screen and a ZnS-Ag screen. The intensity is given along the vertical axis on the left on an arbitrary scale. The dotted line represents the relative spectral sensitivity of a non-sensitized photographic film, derived from measurements with Agfa Spectral and Ilford Spec. Rapid films; the corresponding scale is given on the right..

Sulphides are apt to give a troublesome phosphorescence, but this can be suppressed by adding a trace of nickel (a so-called "killer") to the luminescent substances.

If it is desired to photograph a viewing screen then the sensitivity of the photographic material must correspond to that of the eye, which means that orthochromatic or panchromatic material must be used. If, however, it is not necessary for the screen to be viewed directly and only screen image photography is to be applied, or if direct photographs are to be taken with an intensifying screen then a non-sensitized film suffices, since there are enough substances to be found which have a powerful emission in the violet or in the near ultraviolet, where this film is most sensitive. For such purposes ZnS-Ag and $CaWO_4$ are suitable.

With the aid of the data given in this article we shall try to decide which of these two substances is to be preferred for making intensifying screens. If it is assumed that the values of the constants A and B in equations (7) to (9) differ very little for these two substances, then these factors can be disregarded, and we have to compare the values of kG for these two luminophores.

Fig. 4 gives μ as a function of λ, while fig. 8 gives G as function of σ/μ and fig. 6 k_{re} as function of λ. By a combination of these data *fig. 11* has been constructed to show the ratio of $(k_{re}G)_{ZnS}$: $(k_{re}G)_{CaWO_4}$ $CaWO_4$ as function of the wavelength. From this figure it is to be seen that with equal values of σ (e.g. 50) and of k_{el} a ZnS-screen yields less energy than one of $CaWO_4$. On the other hand, however, owing to the larger crystals in ZnS-screens the value of σ is usually smaller; moreover, the light emission of ZnS-Ag matches the sensitivity of the photographic plate better (see *fig. 12*). In practice one finds the following conditions [7]):

Tube voltage in kV	Ratio of the amplifying factors ZnS : $CaWO_4$
40	3
55	3
70	2.5
85	1.5
100	1.25

From these figures one will therefore be inclined to prefer zinc sulphide screens to calcium tungstate screens where these are to be used as intensifying screens with low tube voltages, but the fact must be borne in mind that with zinc sulphide screens the X-ray image is less sharp.

This screen-unsharpness, which is inherent in the use of intensifying screens and plays an important part also in viewing screens, will be discussed in a subsequent paper.

---

[7]) Taken from a publication of Ilford Ltd. The figures relate respectively to Ilford Standard Tungstate and Ilford Fluorazur Screens.

A CONDENSER-MICROPHONE FOR STEREOPHONY

by A. RADEMAKERS.

621.395.616 : 534.76

During recent years a condenser-microphone has been employed in Philips laboratory for stereophonic sound reproduction. For this purpose the condenser-microphone has to satisfy certain requirements, viz: 1) up to 14 000 c/s the frequency characteristic must follow a horizontal straight line; 2) the dimensions of the microphone may not exceed the wavelength at the highest frequency to be reproduced; 3) the threshold value must lie below 30 phons (i.e. sounds stronger than 30 phons must come through undisturbed). The first requirement is met by ensuring that the resonance frequency is 12 000 c/s, by utilizing the "stiffness" of the air cushion behind the diaphragm. The resonance peak is eliminated by introducing an air-damping. In order to obtain, with the small dimensions, a sufficiently low threshold value, the distance between the diaphragm and the electrode must be small (13 μ). The sensitivity appears to be 3 mV/μbar for a direct voltage of 100 V. Finally the construction is described.

The various types of microphones

In the course of years many different principles have been applied for the construction of microphones, each of which in turn was popular for a time. First of all the common telephone working on the electro-magnetic principle was used as microphone, but its low sensitivity was a drawback. because there were then no amplifiers available. Then the carbon microphone offered a solution, until the advent of radio broadcasting made heavier demands upon the quality of the microphone, whilst with the employment of amplifiers sensitivity became of less importance. One of the oldest quality microphones consisted of a coil in the shape of a flat helix suspended in the wide air-gap of an electromagnet; this may be regarded as the forerunner both of the coil microphone and of the ribbon microphone, both of which types are still at the present day considered to be first-class microphones and are frequently used.

For quite a time a prominent place was occupied by an improved design of the carbon microphone of much better quality due to its filling of fine-grained carbon powder and large diaphragm. With large volumes, however, the sound was too badly distorted.

A remedy of this evil was found — though at a sacrifice of sensitivity — in the condenser-microphone, which then ousted the carbon microphone. The objection, however, of having to mount the first amplifying valve in the immediate vicinity of the microphone led in turn to the advent of the electro-dynamic microphone, whilst also the piezo-electric principle opened the possibility of constructing good microphones. But all these types of microphones have their typical drawbacks, so that not a single one of them has definitely done away with the others, and thus various types are still in use for different purposes [1]).

The innovation of frequency modulation, accompanied by the aim at extending the frequency characteristic up to the highest tone limit, and, further, the necessity of placing two microphones in a dummy head for stereophonic sound reproduction [2]), led to the desire to restrict the dimensions of the microphone.

As to expansion of the frequency characteristic, when the dimensions of the microphone are larger than the wavelength of the sound and this microphone is introduced into a sound field then the original sound field is disturbed by the occurrence of diffraction phenomena. As a consequence, the actual frequency characteristic of the microphone (so-called field calibration) is different from that obtained when the microphone is exposed to a frequency-independent sound pressure (pressure calibration). Since this is undesirable, it is necessary that the microphone should be smaller, at least in two dimensions, than the wavelength at the highest frequency to be reproduced.

For stereophony a dummy head is used, so that the two microphones pick up the sound with the same differences as are received in the ears of the human head when one is listening normally. It would, therefore, be obvious to choose dimensions for the microphone of the same order as those of the human ear.

Electro-dynamic microphones with their rather voluminous permanent magnet cannot be made sufficiently small. The Rochelle salt crystals used in piezoelectric microphones have certain peculiarities making these microphones less suitable for quality reproduction. We have therefore tried to make the small condensor-microphone that has been in use a long time already for measuring purposes suitable for the reproduction of music. Owing to the limit set in the reduction of the dimensions by the accompanying decrease of sensitivity of the microphone, the dimensions could not actually be kept smaller than the wavelength at the highest frequencies. We have chosen a diameter equal to the wavelength at a frequency of about 14 000 c/s, i.e. 25 mm, so that the active part of the diaphragm may be about 15 mm in diameter. With these dimensions differences may arise between the field and the pressure calibration at frequencies above 2000 c/s, at most 5 db. when sound waves of 14 000 c/s strike the diaphragm perpendicularly; corrections must therefore be made when these microphones are used for measuring purposes.

---

[1]) An exhaustive discussion of various types of microphones is to be found in an article by J. de Boer, Philips Techn. Rev. 5, 140-148, 1940.

[2]) K. de Boer, Stereophonic sound reproduction, Philips Techn. Rev. 5, 107-114, 1940, and Stereophonic images, ditto, 8, 51-56, 1946 (No. 2).

When the microphone is used in a dummy head it is not the dimensions of the microphone that govern the diffraction phenomena but rather those of the dummy head itself. Nevertheless, the diaphragm may not be too large because otherwise different parts of it would be activated in different phases. With the chosen diameter of 15 mm the deviations due to this effect are kept below 2 db.

As already remarked, a reduction in dimensions is accompanied by reduced sensitivity, the latter being understood as the voltage supplied per microbar pressure [3]). In itself this is of little importance because with the present-day amplifying technique it is always possible to amplify a signal to the desired strength. Sensitivity only plays a part in as far as it influences the so-called threshold value of the microphone.

By threshold value is understood the loudness level [4]) of the sound that produces on the output side of the amplifier the same voltage as function of time as the noise of the circuit. It is essential that the weakest sounds to be transmitted should be stronger than the noise of the amplifiers. For that reason this threshold value is a measure for the usefulness of the microphone. It determines the weakest sounds that the microphone can reproduce without interference and should, therefore, really lie below the threshold value of hearing. Since, however, there is inevitably a certain noise level in the studio and in the concert hall, one can safely take the threshold value of the same order as that noise level. For the present we have to be satisfied with a threshold value of 30 phons, though this is higher than what can be reached with some other microphones [5]).

The working of the condenser microphones

The first condenser microphone of the form in which it is commonly used at present was made by Wente [6]) in 1917. This type has a vibrator, facing a fixed elctrode; together they form a condenser. The vibrator must therefore be electrically conductive. It consists of a very thin foil of metal (e.g. aluminium 15 μ thick) stretched taut. *Fig. 1* is a schematic diagram of the arrangement of a condenser-microphone. Owing to the movement of the vibrator the capacitance of the condenser undergoes changes and as the flow of the charge is obstructed by the resistance potential differences arise between the points *A* and *B*.

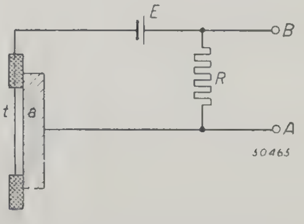

Fig. 1. Diagrammatic representation of the arrangement of a condenser microphone. The flexible electrode or vibrator *t* and the fixed or rear electrode *a* are connected via a resistor *R* to the poles of a battery *E*. The movement of the vibrator causes capacity changes of the condenser which result in voltage variations between the points *A* and *B* of the circuit.

Let us imagine, for simplification, that the resistance is so great as to keep the charge Q of the microphone constant. In that case the voltage V on the microphone will always be inversely proportional to the capacitance C ($V = Q/C$). In order to obtain a horizontal electrical frequency characteristic it is desired that equal sound pressures with different frequencies should give the same variations in capacitance, thus the same movements of the diaphragm. This is the reason why the foil is stretched taut. The resonance frequency is then high, and sufficiently far below this frequency the deviation of a resonator with the same force is independent of the frequency.

---

[3]) 1 μbar sound pressure means an R.M.S. alternating pressure of 1 dyne per cm^2.

[4]) The loudness of the sound is expressed in phons, the given value indicating by how many decibels an equally loud sound of 1000 c/s lies above the intensity of 10^{-16} W/cm^2. A tone of 1000 c/s and a pressure of 1 μbar has a loudness of 74 phons. The noise in a "quiet" concert room amounts to about 34 phons, and a normal conversation corresponds to 60 phons,

[5]) An article will shortly be published in this journal on a circuiting scheme worked out in Philips laboratory which when applied to the condenser-microphone gives a very low noise level.

[6]) E. C. Wente, Physical Review, **10**, 39-63, 1917.

In the case of a simple resonator having the mass m and stiffness s, upon which a sinusoidal force acts which varies with the time t and has the amplitude K, the equation of motion applying is:

$$m\ddot{x} + sx = K \sin \omega t,$$

where ω represents the angular frequency of the force. Resonance occurs when $\omega_0 = \sqrt{s/m}$, whilst when $\omega < {}^1/_2\, \omega_0$ with a deviation less than 2 db

$$x = \frac{K}{s} \sin \omega t.$$

From this it follows that with frequencies sufficiently far below the resonance frequency the unloaded microphone will give a horizontal characteristic. Confining ourselves to this area, we shall give farther on in this article a calculation of the sensitivity of the microphone, when it will be shown at the same time how the non-linear distortion is restricted to imperceptible values. This will be followed by a discussion as to how the horizontal part of the frequency characteristic can be extended to higher frequencies, whilst finally we shall deal with the influence of the electric circuit. We then have to do with the case where the microphone is working under load, a state which influences the frequency characteristic. Moreover, the circuiting involves noise voltage, which affects the threshold value of the combination of microphone and amplifier.

Calculation of sensitivity

When we regard the diaphragm as a simple resonator we must assume that its deflection can be described with one coordinate. This is indeed possible as long as the frequency does not go far beyond that of the first resonance and all points of the diaphragm therefore move in phase with a practically constant characteristic deflection.

If this characteristic deflection is known then an equivalent amplitude can be ascribed to it, for instance by determining the average of the amplitude over the whole area (O). One then finds the equivalent mass m_{eq} and the equivalent stiffness s_{eq} of the system with one degree of movement by writing the kinetic and potential energies of the diaphragm proper respectively as

$$E_K = {}^1/_2\, m_{\text{eq}} \cdot \dot{x}^2_{\text{eq}} \qquad \text{and} \qquad E_P = {}^1/_2\, s_{\text{eq}} \cdot x^2_{\text{eq}}.$$

The force exercised upon the diaphragm by the sound pressure p has an equivalent value equal to the actual force $p \cdot O$, since the work performed for a certain deflection can be written directly as the product of the actual force and the average deflection.

If we regard the metal foil as being entirely without any bending stiffness, thus as a stretched ideal diaphragm, then the deflection curve is fairly easily calculated. When a constant pressure is applied on one side (thus for the static case) the deflection is parabolic, whilst for the first characteristic vibration it is in the form of a Bessel function J_0.

The table below gives for these two cases:

1) the amplitude x as function of the distance ϱ to the centre (R = radius of the diaphragm),
2) the maximum amplitude x_0 (for $\varrho = 0$) divided by the average amplitude $\bar{x}$,
3) the resultant m_{eq} divided by the actual mass m.

$x(\varrho)$	$x_0/\bar{x}$	m_{aeq}/m
$x_0\left(1 - \frac{\varrho^2}{R^2}\right)$	2	1.33
$x_0\, J_0\left(2.4 \cdot \frac{\varrho}{R}\right)$	2.32	1.45
average:	2.16	1.4

The actual shape of the curve is not easy to describe. In the first place the bending stiffness of the material undoubtedly plays a part. This rigidity tends to concentrate the deflection towards the centre, so that $x_0/\bar{x}$ rises (we have in mind here a flat clamped edge). On the other hand, however, there is the influence of the air between the diaphragm and the electrode, which tends to restrict most the greatest amplitudes and thus to reduce $x_0/\bar{x}$; this factor will be discussed later on.

We take it, therefore, that the figures given in the table above do not differ much from the reality, and we can now make an approximate calculation of the sensitivity of the microphone in order to form an idea of the order of size of the actual figures.

An aluminium foil with a diameter of 15 mm and thickness of 15 μ has a mass of about 7 mg. This gives an equivalent mass of $7 \times 1.4 = 10$ mg. If this is to have a resonance frequency ν of 12 000 c/s then an equivalent stiffness is needed of $5.6 \cdot 10^7$ dyne/cm = 5.6 kg/mm. With a sound pressure of 1 μbar (which at 1000 c/s corresponds to a loudness of 74 phons) the equivalent force acting upon the diaphragm is 1.8 dynes. The r.m.s. value of the average amplitude is then $1.8/5.6 \cdot 10^7$ cm = 3.2 Å.

This is of the order of the spacing of the atoms in a crystal. It is astonishing that the microphone should still be able to give undisturbed reproduction with a 100 times smaller amplitude (34 phons) in spite of the fact that the movements of the diaphragm are then smaller than the dimensions of the atoms.

With the strongest sound occurring the amplitudes are 200 times greater than the first mentioned value.

The peak value of the deflection in the centre of the diaphragm is then 0.13 μ, which is still to be regarded as small compared with the distance *a* between the diaphragm and the fixed electrode, which usually exceeds 10 μ and in our case amounts to about 13 μ.

We shall now calculate the capacitance between the diaphragm and the electrode for the case of a parabolic deflection with an amplitude x_0 in the centre and thus $^1/_2 x_0$ as average value:

$$C = \int_0^R \frac{2\pi\varrho \cdot d\varrho}{4\pi\left[a + x_0\left(1 - \frac{\varrho^2}{R^2}\right)\right]} = \frac{O}{4\pi a}\left(1 - \frac{1}{2}\frac{x_0}{a} + \frac{1}{3}\frac{x_0^2}{a^2} - \ldots\right).$$

If the diaphragm is considered as one flat plane displaced with the average amplitude $^1/_2 x_0$ then the capacitance would be:

$$\frac{O}{4\pi a\left(1 + \frac{1}{2}\frac{x_0}{a}\right)} = \frac{O}{4\pi a}\left(1 - \frac{1}{2}\frac{x_0}{a} + \frac{1}{4}\frac{x_0^2}{a^2} - \ldots\right).$$

Since x_0/a is always less than 1% the variation in capacitance (which in both series is represented by the terms containing x_0) can be determined within an error of less than 2‰ by assuming that the diaphragm vibrates as one flat plane with the given amplitude.

In our microphone the fixed electrode has a diameter of 12 mm, thus smaller than the diaphragm, for reasons of insulation. For the variation in capacitance we have only to reckon with this part of the diaphragm. If we take for this x_0 divided by the average amplitude we find $x_0/\bar{x} = 1.4$. The average amplitude of 3.2 Å for the whole diaphragm thus corresponds to an average of 4.5 Å taken over the active part.

If we assume that the charge of the microphone remains constant and that the voltage between the diaphragm and the fixed electrode is 100 V (any higher voltage involves the risk of shorting) then for the amplitude mentioned we arrive at a calculated alternating voltage of 3.5 mV, since with constant charge and thus constant field strength the voltage varies proportionately with the distance. This voltage value agrees well with the measured value of the sensitivity.

Damping and air-rigidity

In the foregoing we have already mentioned that the resonance frequency of the diaphragm is 12000 c/s. This has been arrived at as a compromise between two requirements, viz:

a) that frequencies up to 14 000 c/s must be reproduced with a reasonably horizontal characteristic (deviations less than 2 db);

b) that the threshold value should lie below 30 phons and sensitivity should be sufficiently high to attain this.

The first requirement could easily be satisfied by choosing a resonance frequency higher than 14 000 c/s, but the higher stiffness that this would require would reduce the sensitivity too much to be able to maintain the second requirement.

We therefore followed another method, fixing the resonance frequency in the highest range to be reproduced and damping off the resonance peak in such a way that the characteristic extends horizontally to 14 000 c/s with only small deviations.

When a diaphragm of duralumin of the dimensions already quoted is stretched as tightly as is possible without fracture, the resonance frequency lies approximately at 8000 c/s. This can be raised to 12 000 c/s in one of two ways, viz:

a) The bending stiffness could be increased by using a thicker material. This, however, means increasing the mass and then the stiffness would have to be further increased; this has a very adverse effect upon the sensitivity.

b) A better method is to arrange for the space behind the diaphragm to be so small that the movement of the diaphragm causes a perceptible compression of the enclosed air, thereby providing additional rigidity.

One might go even as far as to consider using a very thin and thus light diaphragm, and deriving the whole of the rigidity from the air pocket. This would, it is true, improve the sensitivity, but on other grounds it is less desirable: the high voltage between the diaphragm and the electrode constitutes an attractive force between the two, with the result that in the event of a small leak in the air chamber there would be a danger of the diaphragm being drawn back onto the electrode. Now it is essential to have such a small leak, in order to avoid a variation in the distance between the diaphragm and the electrode due to gradual barometric changes. We have therefore kept to a diaphragm 15 μ thick.

If the volume of air behind the diaphragm were to consist only of the approximately 13 μ thick layer between the diaphragm and the electrode, the air rigidity would be fantastically high, as is evident from what follows.

A movement of the diaphragm over a distance $\bar{x}$ then gives, with adiabatic compression, a rise Δp of the pressure p according to the equation:

$$\frac{\Delta p}{p} = -\frac{\Delta V}{V} = -\varkappa\frac{\bar{x}}{a}.$$

where V is the volume of air and $\varkappa$ is the ratio of the specific heat of air under constant pressure to that for constant volume ($\varkappa = 1.4$). The force required (apart from the sign) is therefore:

$$\Delta p \cdot O = \bar{x}\frac{p \cdot \varkappa \cdot O}{a},$$

and the stiffness is

$$s_{\mathrm{aeq}} = \frac{p \cdot \varkappa \cdot O}{a}.$$

With $p = 1$ atm $= 10^6$ dyne/cm² and $a = 13 \cdot 10^{-4}$ cm we therefore get:

$$s_{\mathrm{aeq}} = 2 \cdot 10^9 \text{ dyne/cm},$$

corresponding to a resonance at 72 000 c/s.

Obviously, in order to reduce the air rigidity the volume of air must be increased, not by increasing the distance a (this would greatly reduce again the generated voltage) but by providing a separate compression space in the form of an annular channel around the electrode or as grooves or cavities in the surface.

The choice of form of this separate compression space is closely related to the damping required for flattening out the resonance peak, because for this damping we make use of the viscous flow of the air in the narrow gap between the diaphragm and the electrode from and to the compression space. Assuming that the air during this flow behaves as if it were incompressible, it is not difficult to calculate the damping action.

In the differential equation now applying for the diaphragm movement,

$$m\ddot{x} + r\dot{x} + sx = K \sin \omega t,$$

we find for the coefficient r in the case of a round flat electrode with radius R and surface O:

$$r = \frac{1.5 \cdot 10^{-3}}{2\pi} \cdot \frac{OR^2}{a^3}.$$

The degree of damping can be judged by calculating $\omega_0 \cdot r$ (ω_0 is the frequency at which resonance occurs). Resolution of the differential equation shows that $\varkappa = K/s$ for $\omega \ll \omega_0$ and $\varkappa = K/\omega_0 r$ for $\omega = \omega_0$. We therefore get the right damping approximately when

$$\omega_0 \cdot r = s.$$

In our case ($R = 0.6$ cm), when $\omega_0 = 2\pi \cdot 12\,000$ c/s is chosen

$$\omega_0 \cdot r = 3.6 \cdot 10^9 \text{ dyne/cm}.$$

This is much too high a value, since the value found above as being required for the equivalent stiffness is $5.6 \cdot 10^7$ dyne/cm.

It is therefore necessary to reduce the resistance by a factor of 150. The formula given for the resistance shows that we can easily do this by dividing the electrode into parts with smaller dimensions. The resistance is then reduced (for the same total area) by the square of those dimensions, When it has been reduced to the desired value ($r = s/\omega_0$) the air is practically incompressible in its flow from and to the grooves in the divided electrode. The rises in pressure in those grooves then react upon the diaphragm and thus produce the additional stiffness required to raise the resonance.

We have divided up the electrode by milling straight grooves in its surface. This results in a somewhat different value for the damping constant, viz:

$$r = \frac{4.3 \cdot 10^{-3}}{2\pi} \cdot \frac{O\,(^1/_2\, b)^2}{a^3},$$

where b is the width of the dam between two grooves.

Although this formula does not yield exact results it is very useful in practice as giving the right relation between the damping and the various dimensions. With the aid of this formula and one experimental model it is generally possible to determine the exact shape the rear electrode should have.

The electric circuit

When we come to consider more closely the manner in which the alternating voltage is generated by the movement of the diaphragm we start from the simplified model: a diaphragm moving to and fro as a flat plane. The capacitance in the position of rest is $C_m = O/4\pi a$, whilst the variations are described by replacing a by $a\,(1 + \alpha)$, where $\alpha = \bar{x}/a$ may, for instance, vary sinusoidally with time. Parallel to the capacitance of the diaphragm is an inevitable scattering capacitance and possibly also a parallel capacitance purposely introduced; these two together are termed C_p.

If we again assume a constant charge then

$$V = \frac{Q}{C_p + \dfrac{C_m}{1+a}} = \frac{Q}{C_m + C_p} \cdot \frac{1+a}{1 + a\dfrac{C_p}{C_m + C_p}} =$$

$$= V_0 \frac{1+a}{1 + a\dfrac{C_p}{C_m + C_p}}$$

invariably applies, in which V_0 represents the voltage in the position of rest.

The voltage variation is

$$\varDelta V = V - V_0 = V_0\, a \cdot \frac{C_m}{C_m + C_p} \cdot \frac{1}{1 + a\dfrac{C_p}{C_m + C_p}} =$$

$$= V_0 \cdot a \cdot \frac{C_m}{C_m + C_p}\left(1 - a\frac{C_p}{C_m + C_p} + \ldots\right).$$

From the formula we see that:

1) the voltage generated is proportional to V_0 and in the first instance proportional to $a = \bar{x}/a$;
2) when a parallel capacitance is introduced the voltage generated is reduced in the ratio $C_m/(C_m + C_p)$;
3) when C_p is introduced there also arises a distortion factor of the order of $a\, C_p/(C_m + C_p)$.

With very strong sound this distortion factor reaches at most a value of 1%, even with a very large C_p/C_m (because we always have $a \ll 1\%$), so that it is negligible in comparsion with the distortion generally occurring in the remaining part of an apparatus for sound transmission.

So far we have been assuming that the microphone has a constant charge, presuning the charge resistance to be high enough. This point, too, has to be looked into more closely.

Without parallel capacitance and with constant charge the microphone produces an "open voltage" $= V_0 a$. When the microphone is connected to the direct voltage source without any resistor in between we get a "shorting current" $= V_0 \cdot dC/dt = V_0 \cdot a \cdot j\varphi C_m$ (when a is taken to be sinusoidal and terms of a higher order are ignored). According to Thévenin's theorem we may consider the microphone as a voltage source of a strength $V_0 a$ with an internal impedance equal to the open voltage divided by the shorting current, thus $= 1/j\varphi C_m$, which is the specific impedance of the microphone. This is indicated diagrammatically in *fig. 2*. With the aid of this result let us consider further how the combination of the microphone with the parallel capacitances and the resistor behaves. In the diagram given in fig. 2 the alternating voltage across R is

$$V_R = a V_0 \frac{C_m}{C_m + C_p} \cdot \frac{1}{1 + \dfrac{1}{j\omega R\,(C_m + C_p)}}.$$

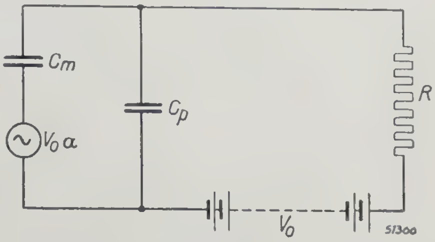

Fig. 2. The electrical circuiting of a condenser microphone in the form in which it might be regarded according to Thévenin's theorem. V_0 is the voltage of the current source, R the resistor, C_m the capacity of the condenser-microphone in the state of rest, C_p the parallel capacity, and a the factor determining the change in the distance between the diaphragm and the rear electrode.

In *fig. 3* this voltage is plotted in its absolute value as a function of $RC_0\omega$, in which $C_0 = C_m + C_p$. We see that for $RC_0\omega \gg 1$ practically the full calculated voltage occurs at the ends of the resistor. At $RC_0\omega = 1$ the signal is reduced by 3 db.

If the lowest frequency to be reproduced is put at $v = 32$ c/s and we allow here a drop of 3 db then we must have

$$R\,(C_m + C_p) = \frac{1}{2\pi \cdot 32} \approx \frac{1}{200} \text{ sec.}$$

This can be attained in various ways, the simplest of which is to choose, for the capacity of the microphone, such a resistance as will satisfy the condition set. This, however, leads to very large resistances (80 megohms, because $C_m = 55$ pF and $C_p = 10$

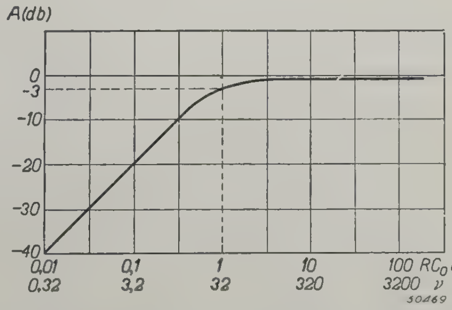

Fig. 3. The relation between the amplitude A of the voltage at the ends of the resistor R and the values of the product $RC_3\varphi$, when the total capacitance is expressed as $C_m + C_p = C_0$ and the angular frequency as φ. These latter values are plotted logarithmically on the x-axis, whilst the voltage is expressed in a decibel scale. For $C_0\varphi = 1$ it is found that $A = -3$ db. The values on the abscissa, expressed in the frequency v, are also given for $RC_0 = 1/200$ sec.

pF at least), and this makes heavy demands upon the insulation both in the microphone and on the grid of the first amplifying valve.

Another solution is to use a resistance not quite so high and to connect a capacitor in parallel to the microphone, but this causes the voltage to drop in the ratio $C_m/(C_m + C_p)$. It is true that a reduction in the resistance causes also a reduction in the noise voltage, but in this case the threshold value is adversely affected, whilst it has to be borne in mind that the noise voltage of the resistor is reduced only in proportion to the square root of the resistance ratio.

A third solution could be found by applying a feed-back voltage in the manner of the much used "cathode-follower", which makes the circuit appear to have a high input resistance. Unfortunately it is found that the ratio of noise to signal is not proportionately reduced, so that this sysem does not offer any real advantage and has the drawback that the first valve does not contribute anything to the amplification.

We have calculated the ratio of the noise voltage to the signal voltage for two cases.

If the resistance R is high (80 megohm) and the parallel capacitance is a minimum (about 10 pF) we find for the signal voltage 3 mV/μbar, A calculation of the r.m.s. value of the noise voltage gives as result 6.0 μV, so that this lies 54 db below the signal voltage at 1 μbar. If there were an interference voltage of this value with a frequency of 1000 c/s this would lead to a threshold value of 20 phons. Taking into account the sensitivity curve of the ear, it is evident that the noise voltage mentioned results in a threshold value lower than 20 phons.

In the second case let $R =$ 5 megohm and C_p = 1000 pF. The signal voltage is then 0.15 mV per μbar. Under these conditions the r.m.s. value of the noise voltage lies 40 db lower than the signal voltage per μbar, namely at 1.4 μV. With a frequency of 1000 c/s of the noise tone the threshold value would then lie at 34 phons; actually it is lower than this.

From this it follows that a satisfactory threshold value can be reached if a sufficiently large resistor is used.

The practical construction

It has already been shown that a combination of an extended horizontal frequency characteristic and a low threshold value can only be obtained by using a diaphragm as light as can be allowed on the aforementioned grounds and with the smallest possible distance between the electrode and the diaphragm as is practicable for manufacturing with a sufficient degree of uniformity. This distance must be kept as uniform as possible because the damping varies according to the third power of that distance; with distances of the order of 10 μ an increase of 1 μ causes a variation in the damping of more than 2 db, which manifests itself in an equally large elevation of the characteristic at the point of resonance. We have not, therefore, attempted to make the distance smaller than that mentioned, the more so because that would make it still more difficult to keep the microphone free of short-circuiting in consequence of extremely small foreign particles.

Fig. 4 gives the frequency characteristics of three microphones with the same electrode but different distances between the diaphragm and the electrode. It appears that this distance is of great importance for the damping and thus for the shape of the characteristic. Graph *a* shows that the damping is too strong, and graph *c* that there is too little damping.

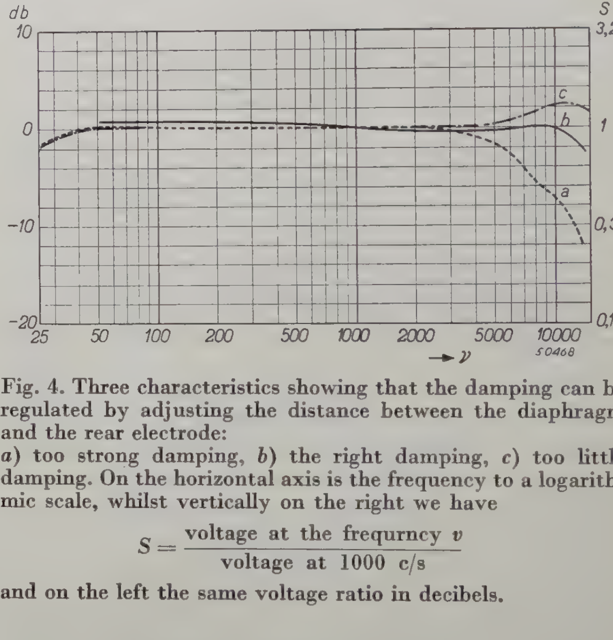

Fig. 4. Three characteristics showing that the damping can be regulated by adjusting the distance between the diaphragm and the rear electrode:
a) too strong damping, *b*) the right damping, *c*) too little damping. On the horizontal axis is the frequency to a logarithmic scale, whilst vertically on the right we have

$$S = \frac{\text{voltage at the frequrncy } v}{\text{voltage at 1000 c/s}}$$

and on the left the same voltage ratio in decibels.

Fig. 5 is a cross-sectional drawing of the condenser microphone as constructed in the Philips laboratory after consideration of the factors dealt with in the foregoing.

The diaphragm is stretched tight in the microphone casing between two rings pressed tightly up against each other by means of a nut. The electrode is pressed into another ring provided with an insulation of amber. The whole is slipped into the microphone and by means of a special nut the electrode ring is forced up until it presses out the diaphragm to get the required tension. It is previously arranged that the surface of the electrode comes to lie 10 μ lower than the rim of the ring into which it is pressed. Finally the electrode is connected to an insulated plug pin.

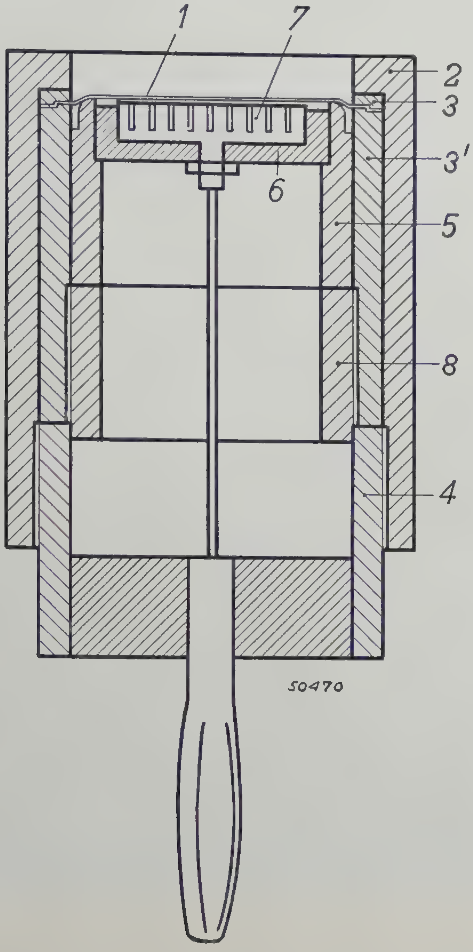

Fig. 5. Cross-sectional drawing of the new design of condenser-microphone, The diaphragm *1* is stretched in the casing *2* of the microphone between the rings *3* and *3′*, which are presesd together by the nut *4*. The rear electrode *7* is pressed into a ring *5* containing an amber insulation *6*. The whole is slipped into the microphone and pressed down until the ring *5* presses through the diaphragm far enough to give the required tension, this being adjusted by means of the nut *8*. It is previously arranged that the surface *7* lies 10 μ below the edge of *5*. The rear electrode is connected to an insulated plug pin.

The following details are given regarding the construction of the electrode system. The electrode proper, which is 12 mm in diameter, is first provided with the required number of grooves (15 grooves 1.8 mm deep and 0.15 mm wide), then placed in the amber ring, after which the whole is pressed into the holder ring; the top edge of the amber ring is then about 0.1 mm below the upper surface of the electrode. The surface of the electrode is then turned on a precision lathe until it comes to lie on a level 10 μ lower than the edge of the holder ring.

This last process has to be done very carefully. If it were done by hand the chisel would make the surface too rough, with the risk of short-circuiting. The chisel has to be driven, with a very small pitch, by a special motor. The displacement of the chisel parallel to the bed over a distance of 10 μ is usually done by hand and is read from a dial gauge mounted on the support. When the surface has been turned any small burrs are rubbed off with a chamois-leather.

The lateral movement of the chisel must of course be absolutely perpendicular to the axis of the lathe, as otherwise the surface would be conical and give rise to short-circuiting or else make the air-gap too large. As a check for accuracy a turned surface was placed underneath an interferometer plate. The tolerance was found to be less than 1 μ over a distance of 15 mm.

Fig. 6 illustrates some specimens of the condenser-microphone.

A good idea of the mechanical accuracy reached can be formed when imagining the microphone to be enlarged 1000 times. The electrode then has a diameter of 12 meters, whilst parallel to it at a distance of 10 mm is a plate 15 mm thick. Capacity measurements have shown that this plate is not absolutely flat but somewhat convex. If the model just described is to answer fully the actual requirements then the distance between the electrode and the plate should be in the middle about 13 mm. This convex shape of the diaphragm is undoubtedly obtained from the pressing in of the duralumin foil when mounting the electrode in the microphone.

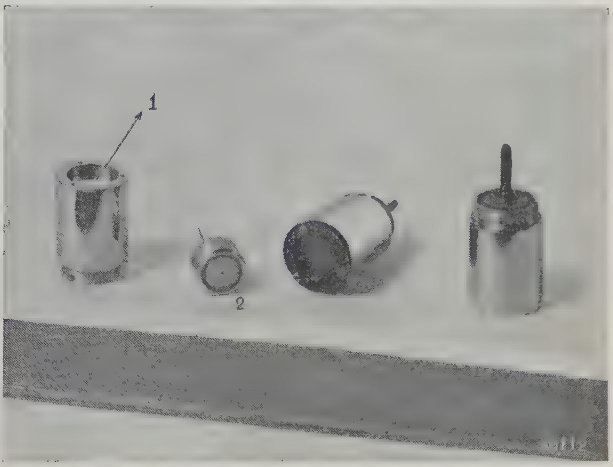

Fig. 6. Some condenser-microphones. The instrument on the left contains the diaphragm *1* stretched in the casing, and beside that is a rear electrode *2*. The microphone lying on its side has a protective gauze over the diaphragm. The ruler gives an idea of the dimensions.

A good idea of the vibration of the diaphragm is obtained from a calculation of the velocity. With a sound pressure of 1 μbar and a frequency of 50 c/s the maximum velocity is:

$$v_{\max} = 2\pi \cdot 50 \sqrt{2{\cdot}4.5{\cdot}10^{-4}}\ \mu/\mathrm{sec} = 1.72\ \mathrm{cm/day}.$$

By way of comparison it may be mentioned that a sunflower grows 2-3 cm per day.

The condenser-microphone described here is being used in the Philips laboratory in the dummy head for experiments in stereophony. It is not precluded that this instrument will find application also for the monaural reception of sound when the desirability of extending the frequency range beyond 10^4 c/s becomes urgent. The objection of the first amplifier having to be set up in the immediate vicinity of the microphone will then have to be overcome in some way or other [7]). The graph in fig. 4 already shows that the quality of reproduction satisfies high demands. Practice has proved that this design can be made with sufficient uniformity for the microphones to be safely interchangeable.

---

[7]) A solution of this problem will be given in the article referred to in footnote [5]).

TELEVISION TUBE PRODUCTION

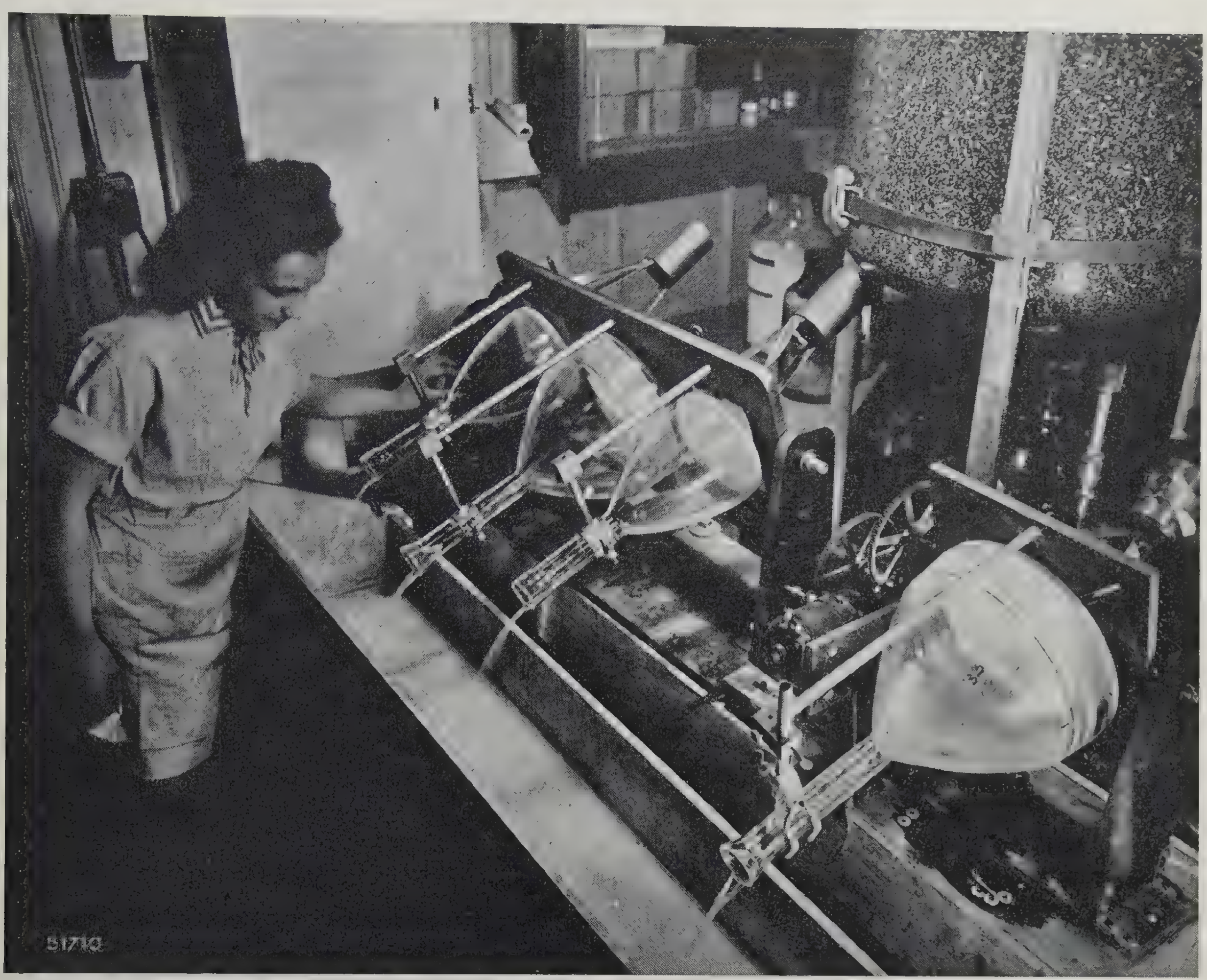

The phosphor coating constituting the fluorescent screen in television tubes is deposited on the face of the tube by settling from a dispersing liquid. The remaining liquid must be removed in such a way as to avoid even the slightest turbulence that would tend to make the liquid wash away parts of the screen. In the Dobbs Ferry, N.Y., plant of North American Philips Co., Inc., the tubes are emptied by tilting them at a slow, uniform rate by means of a carefully balanced machine operated by a small electric motor and gear system.

AN ELECTRONIC SWITCH WITH VARIABLE COMMUTATING FREQUENCY

by E. E. CARPENTIER. 621.317.755.06

A description is given of a new construction of an electronic switch (type number GM 4580) for the simultaneous production of two oscillograms. Various steps have been taken to avoid disturbing peaks in the output voltage. The normal oscillograph amplifier, which led to distortion of the commutating voltage, is no longer used (except as pre-amplifier for one of the voltages to be imaged). As a result it has been possible to raise the commutating frequency to 40 000 c/s, thereby improving the clearness of the details in the oscillograms. Moreover, this frequency is continuously variable, to 2 c/s downwards, which in certain cases is of advantage. The input may be asymmetrical or symmetrical as desired, the latter being useful, *inter alia,* when it is desired to produce more than two oscillograms simultaneously with the aid of electronic switches in cascade.

With the aid of a cathode-ray oscillograph ¹) the trend of a voltage can be pictured as function of another voltage. If for the latter a linear time-base voltage is used then the screen of the oscillograph shows the trend of a voltage as a function of the time. Although in many cases it is not required, it is often desirable to produce an image of two or more voltages simultaneously as functions of some other voltage, for instance when it is required to record or measure a difference in time or phase.

In a method already frequently described in literature — also in this journal ²) — a switch is used which connects the two voltages to be oscillographed alternately to the plates for the vertical deflection in a normal oscillograph; here the switching is effected by means of electronic valves.

Principle of the electronic switch

The principle of such an electronic switch is recalled with reference to *fig. 1*, relating to an earlier design of such an apparatus (*cf.* footnote 2). The voltages to be oscillographed v_I and v_{II} are conducted to the channels *I* and *II* of the electronic switch, the inputs of which are connected to the control grids of the pentodes P_I and P_{II} respectively. The two screen grids of these pentodes are connected to mutually phase-opposed alternating voltages having an approximately rectangular curve. These so-called commutating voltages are generated by a multivibrator on the Abraham and Bloch principle: their amplitudes are such that alternately one of the pentodes is in the normal working state while the other is dead. The current in the common anode resistor R_a thus flows alternately through P_I or P_{II}; consequently this current — and thus also the anode voltage — is alternately governed by v_I or v_{II}. The anode voltage governs in turn (*via* an amplifier) the vertical deflection of the oscillograph.

The time during which the commutating voltage oscillates is chosen small in respect to the time taken by the spot of light to traverse the screen from left to right. A picture is then produced of the nature of that shown in *fig. 2* (where for the sake of clarity the commutating frequency has been chosen much too low). Each of the image curves is thus a dotted line.

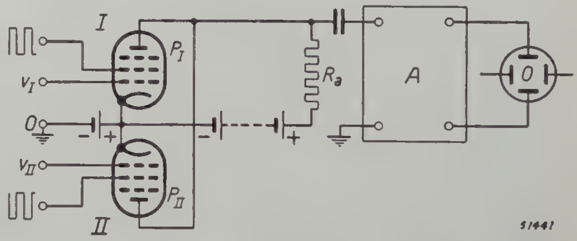

Fig. 1. Circuiting diagram of an electronic switch. *I* and *II* are channels functioning alternately for carrying the input voltages v_I and v_{II} to the amplifier *A* and the oscillograph tube *O*. P_I and P_{II} are pentodes, R_a is a common anode resistance.

By another and perhaps more obvious method of producing two or more oscillograms simultaneously an oscillograph tube is used in which a number of electron beams each describe an oscillogram on the screen. The tube contains the same number of cathodes — each with its appropriate focusing, accelerating and deflecting system — as the number of oscillograms it is desired to record simultaneously. The fact that in this way continuous lines are produced instead of dotted lines (fig. 2) has the advantage, *inter alia,* that no details are lost in the oscillograms and the luminous intensity obtained from one beam of electrons is not distributed over a number of curves. There are, however, also some objections, such as the unavoidable differences between the deflecting systems (small differences in sensitivity, for instance, may be very troublesome). Further, especially at high frequencies, there will

---

¹) For descriptions of cathode-ray oscillographs see inter alia: Philips Techn. Rev. **1**, 147-151, 1936, (type GM 3150), Philips Techn. Rev. **4**, 198-204, 1939, (type GM 3152), Philips Techn. Rev. **5**, 277-285, 1940, (type GM 3156), Philips Techn. Rev. **9**, 202-210, 1947, No. 7 (type GM 3159).

²) C. Dorsman and S. L. de Bruin, An Electron Switch, Philips Techn.Rev. **4**, 267-271, 1939.

be mutual reactance between the deflecting systems. But it is mainly the complexity of the construction that has prevented these multiple tubes from becoming more generally employed.

Upper limit of the commutating frequency

The higher the commutating frequency is chosen, the finer is the structure of the image, so that smaller details can be reproduced. There is, however, a limit to the raising of this frequency, at least when the output voltage of the electronic switch is so small as not to be able to dispense with the amplifier of the oscillograph, for it is then necessary that this amplifier should amplify a rectangular oscillation without any distortion; this means that it must produce a large number (*e.g.* 100) of harmonics with reasonably faithful amplitude and phase. With the amplifier of a normal oscillograph, for instance of the type GM 3152, one arrives at a maximum commutating frequency of 8 000-10 000 c/s, which value is therefore used in the electronic switch (type GM 4196) described at the time in the article referred to in footnote 2.

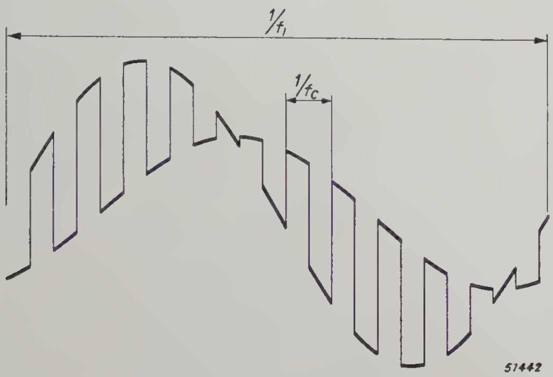

Fig. 2. Picture of two sinusoidal input voltages as it appears on the oscillograph with the circuiting according to fig. 1 when the commutating frequency f_c is higher than the frequency f_i of the input voltages. In reality f_c is much higher than is represented here.

The fact that the shape of the curve of the commutating voltage obtained with this apparatus after amplification still leaves much to be desired is to be seen from *fig. 3a*; here the two input voltages were zero. This is manifest in the oscillograms produced with such a commutating voltage, as seen for instance in fig. 3*b*; the peaks visible in fig. 3*a* fog the image.

In the designing of the new electronic switch (type GM 4580) to be described below the object has been to improve the quality of the oscillograms as far as possible, for instance by giving the amplified commutating voltage a shape more closely approaching a rectangle. *Fig. 4a* shows the oscillogram of this voltage and fig. 4*b* an oscillogram produced with it. A comparison of fig. 4*b* and fig. 3*b* clearly shows that the troublesome fogging has been eliminated.

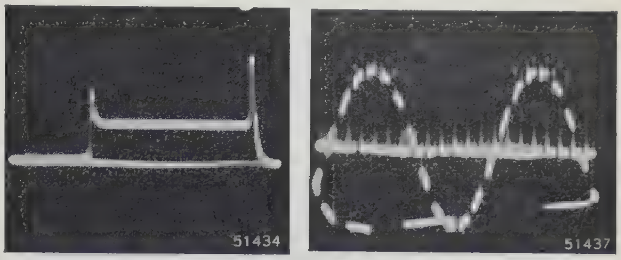

a *b*

Fig. 3. *a*) Oscillogram of the output voltage of the amplifier of the oscillograph GM 3152 with the old electronic switch GM 4196 connected in front of it, the two input voltages of the latter being zero. The voltage obtained (frequency about 8000 c/s) deviates rather considerably from the rectangular shape, this being due, *inter alia*, to a peak arising at each commutation.

b) Oscillogram of a voltage with a frequency of about 600 c/s and a zero voltage recorded with the combination of GM 4196 and GM 3152. The peaks visible in (*a*) cause a troublesome fogging of the picture.

Improved electronic switch

The main points of difference between the electronic switch GM 4580 illustrated in *fig. 5* and its predecessor are the following:

I) The amplified commutating voltage (*i.e.* the voltage on the oscillograph plates when both input voltages of the electronic switch are equal direct voltages) no longer has the disturbing peaks previously referred to. Distortion in the oscillograph amplifier is avoided by dispensing with the use of that amplifier (except as pre-amplifier for one of the voltages to be imaged, to which we shall revert later).

II) The commutating frequency has been made variable. On the one hand it can be raised to 40 000 c/s, so that four times as small details

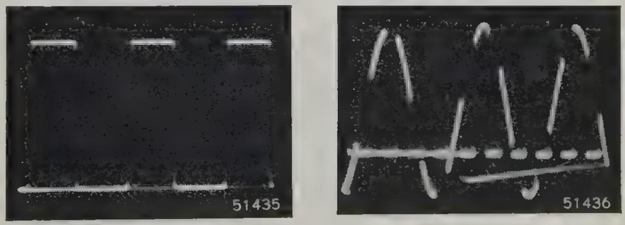

a *b*

Fig. 4. *a*) Oscillogram of the output voltage of the new electronic switch GM 4580 (both input voltages zero); here the frequency was again about 8000 c/s. The rectangular shape is much more closely approximated than in fig. 3*a*.

b) Oscillogram of a voltage with a frequency of about 2000 c/s and a zero voltage recorded with the combination GM 4580/GM 3152.

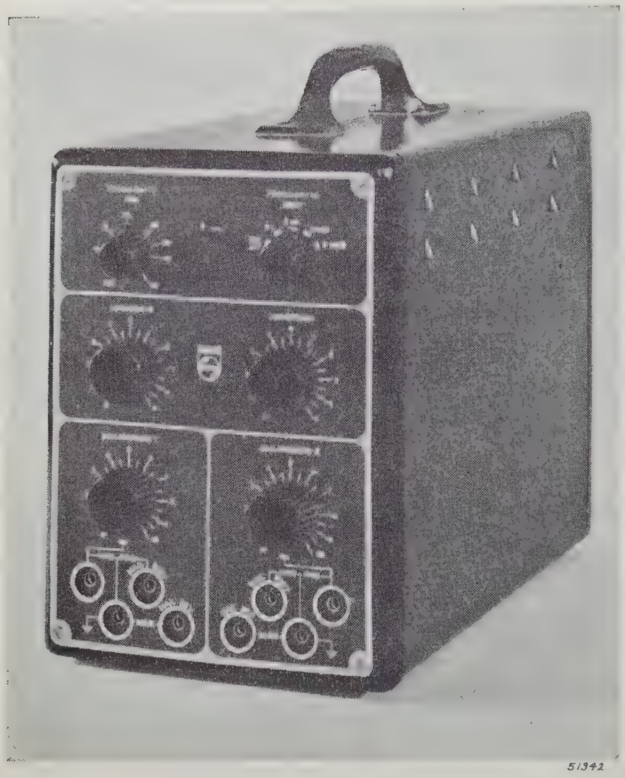

Fig. 5. The new electronic switch type GM 4580. From top to bottom: two knobs for regulating the commutating frequency, two knobs for vertical displacement of the image (left-hand one for shifting the whole image, right-hand one for shifting the two oscillograms in opposite directions), two knobs for regulating the sensitivity of the channels, terminal sockets for the symmetrical and the asymmetrical inputs.

can be made visible, whilst on the other hand it can be adjusted to extremely low values, which may be advantageous in some cases.

III) The inputs of the electronic switch can be made asymmetrical or symmetrical as desired. The latter is useful, for instance, for the simultaneous production of more than two oscillograms.

These points will be discussed further below.

I) *Avoidance of troublesome peaks and distortion*

One of the causes of the occurrence of troublesome peaks in the amplified commutating voltage lies in the fact that the multivibrator voltage shows a curve with somewhat concave flanks, which is consequently likewise the case with the anode currents of the pentodes in the electronic switch (*figs. 6a* and *b*); this has already been mentioned in the article quoted in footnote 2. For every commutation this gives rise to a drop in the current flowing through the common anode resistor (fig. 6*c*) and a corresponding peak in the anode voltage (fig. 6*d*). We have already seen what these peaks are like in figs. 3*a* and *b*.

By applying a push-pull circuit in both channels of the electronic switch these peaks in the output voltage are avoided. The manner in which the push-pull circuit may be arranged is shown for one channel in *fig. 7* (actually the circuit is somewhat different, as will be seen farther on). In order to obtain an output voltage symmetrical with respect to earth in spite of the fact that the input voltage v_I is asymmetrical, use can be made of the method previously described [3]) where a resistor R_{kI} (fig. 7) is introduced in the common cathode line. As a result when $SR_{kI} \gg 1$ the output voltage is practically symmetrical (S = slope of the valves).

In *fig. 8* this push-pull circuit is applied to two channels. It is also indicated how in each channel the two pentodes in push-pull can be replaced by one double pentode (type EFF 51). The circuit is shown for asymmetrical inputs, but in reality the new electronic switch has also symmetrical inputs; we shall revert to this later.

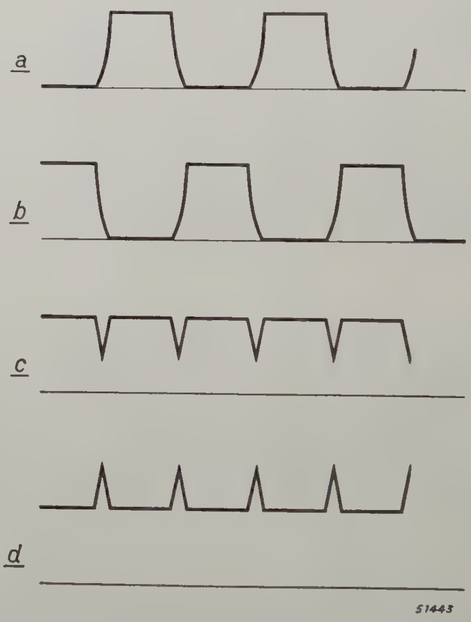

Fig. 6. Trend of the two anode currents (a and b), the current (c) through the resistance R_a and the anode voltage (d) in the circuit according to fig. 1, with equal and constant values of v_I and v_{II}.

It is easily understood that with push-pull circuits the peaks previously referred to will no longer occur, for from fig. 8 it may be seen that if the two input voltages are zero then the output voltage v_o amounts to:

$$v_o = (i_I' + i_{II}')\,R_a' - (i_I'' + i_{II}'')\,R_a'',$$

in which $i_I' \ldots i_{II}''$ represent the anode currents

---

[3]) See the last of the articles listed in footnote 1, in particular fig. 3*b*.

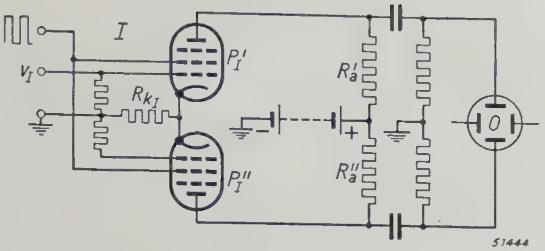

Fig. 7. Here the channel I of fig. 1 is in push-pull (pentodes P_I' and P_I''). R_{kI} is a common cathode resistance ensuring symmetrical action.

of the four pentodes $P_I' \dots P_{II}''$, and R_a' and R_a'' represent the two anode resistors. On account of the approximate symmetry of the push-pull circuits we have at any time $i_I' \approx i_I''$ and $i_{II}' \approx i_{II}''$, so that if $R_a' = R_a''$ the output voltage is indeed approximately zero.

Another cause of undesired peak voltages lies in the capacitive effect exercised upon the control grid by the screen grid to which, in the circuiting described above, a commutating voltage is applied. Every jump in the screen grid voltage results in a current impulse in the circuit formed by the capacitance C_{sg} between the screen and control grids (*fig. 9*) and the impedance Z_g between control grid and cathode. This current impulse gives rise in turn to a voltage impulse on the control grid. When the screen grid voltage jumps from a positive value to zero the corresponding peak on the control grid is of little consequence, since the anode current disappears at the same moment (owing to the screen grid voltage dropping to zero). A jump in the reverse direction, however, is indeed reflected in the output voltage.

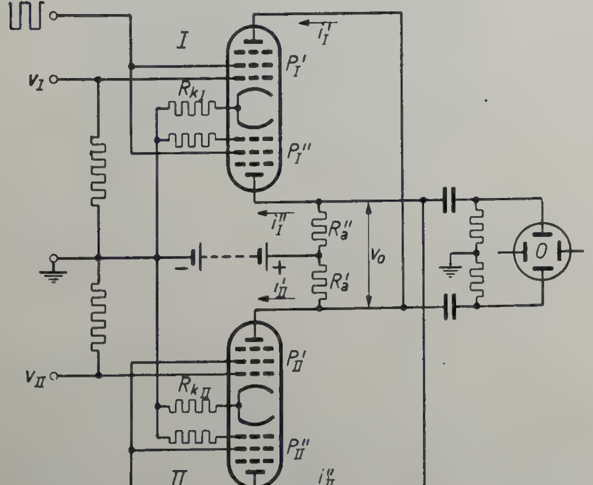

Fig 8. Both channels of fig. 1 in push-pull as indicated in fig. 7 for channel I. The pentodes P_I' and P_I'', respectively P_{II}' and P_{II}'', can be replaced by a double pentode (type EFF 52).

In this case a push-pull circuit as illustrated in fig. 7 cannot alter matters. The amplitude of the disturbing voltage on the control grid depends upon the impedance Z_g; in the control grid circuit of P_I'' this has a fixed value, but in the case of P_I' it is formed partly by an external impedance (that of the source of the input voltage), which may have any value. Consequently there is not as a rule any symmetry such as is obtained in the previous case, with the result that even with push-pull circuits peaks of the kind in question here may still arise.

In the electronic switch of the type GM 4580 this phenomenon is greatly reduced owing to the fact that the commutating voltage, instead of being conducted to the screen grid circuit, is applied to the control grid circuits, parallel to R_k (*fig. 10*). Owing to the presence of the capacitance C_{gk} between control grid and cathode the effect does, it is true, still arise in principle; even more so, since C_{gk} is about twice as large as C_{sg}. But this is amply compensated by the fact that a much smaller amplitude of the commutating voltage is needed on the control grid than on the screen grid, namely 10 V instead of 250 V. As a result the peaks in question become 10 times smaller and are therefore no longer troublesome.

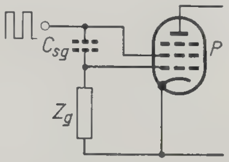

Fig. 9. The commutating voltage on the screen grid of the pentode P causes, *via* the capacitor C_{sg} between the two grids a voltage impulse on the control grid. Z_g = the total impedance between control grid and cathode.

This low value of the commutating voltage has yet another favourable effect, in that the time required for this voltage to rise from the minimum to the maximum value, or *vice versa*, can be kept short. (During these intervals of time the cathode ray does not produce any effective light on the screen, and, moreover, any details of the input voltages happening to occur just in those intervals do not become visible.) The reason why this commutating time is not zero is to be sought mainly in stray capacitances in the multivibrator exciting the commutating voltage. The adverse influence of these capacitances is all the less according as the resistances to which they are connected in parallel have a lower value. The smaller the commutating voltage required, the lower these resistances may be chosen. The fact, therefore, that in the new electronic switch only 10 V suffices (where formely 250 V was needed) leads to a much shorter commutating time. We have gone a step farther in this direction by choosing relatively high anode currents in the multivibrator, thereby lowering the resistances still further. (The multivibrator is equipped with output pentodes of the type EBL 21.)

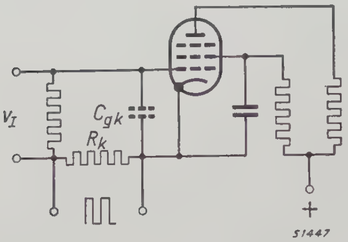

Fig. 10. The commutating voltage is conducted to the resistor R_k in the control grid circuit; the screen grid is fed in the normal manner with a direct voltage. C_{gk} = capacitance between control grid and cathode.

Another important difference between the old electronic switch and the new one is the fact that with the latter no use is made of the normal oscillograph amplifier between the electronic switch and the oscillograph tube, thus avoiding a serious source of distortion of the commutating voltage. In order to get an oscillogram of reasonable height also with relatively small input voltages, it has been arranged for the electronic switch itself to act as an amplifier as well. The amplification cannot, it is true, be raised very high without giving rise to the same difficulties as occur with the normal oscillograph amplifier, but with the amplifying factor of 100 applied here no trouble is experienced in this connection, whilst for many applications the sensitivity is still sufficient. Moreover, there is no objection to the oscillograph amplifier being used as pre-amplifier, placing it in front of one of the channels of the electronic switch, so that a very great sensitivity is available at least on one channel [4]).

The fact that the oscillograph plates for the vertical deflection are now connected directly to the output of the electronic switch constitutes a second argument for applying the push-pull principle in this switch, as otherwise defocusing of the electron beam and distortion of the image would occur [5]).

II) *Variable commutating frequency*

With the dispensing of the amplifier between the electronic switch and the oscillograph tube we have removed the greatest obstacle preventing the commutating frequency f_c from being raised. In the new electronic switch f_c has been made variable — the use of which will be explained presently — with 40 000 c/s as the upper limit, so that the structure of the image obtained is four times finer than was the case with the old type. Furthermore, f_c can be regulated to very low values, it being desirable in certain cases to have a commutating frequency which is low in comparison with the frequency f_i of the voltage to be screened (*fig. 11*). The screen then first shows for a time the complete oscillogram of one voltage, followed by that of the other voltage, then again the first, and so on. There is, however, a limit to which the commutating frequency f_c can be reduced, at least for the visual recording of the oscillograms, because if the transition is too slow there is a troublesome flickering of the image. For this reason f_c should not be chosen lower than about 50 c/s. When the voltage frequency f_i is 1000 c/s or more then as a rule a slow commutation ($f_c \ll f_i$) will yield better results than rapid commutation ($f_c \gg f_i$). If, on the other hand, f_i is lower than about 200 c/s, in order to avoid flickering one must have rapid commutation. In between these limits it does not matter much whether one chooses $f_c \gg$ or $\ll f_i$ [6]).

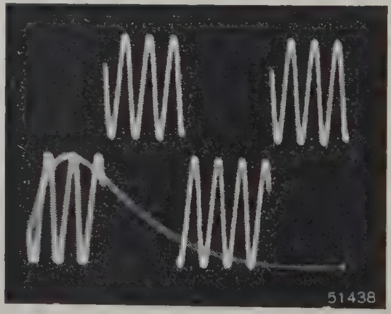

Fig. 11. Oscillograms recorded with a low commutating frequency ($f_c < f_i$). The frequency of the time-base voltage has been chosen low enough for the image to cover two cycles of the commutating frequency.

When the image is photographed this flickering is of no consequence (at least if the exposure time is greater than $1/f_c$; each of the two oscillograms requires the time $^1/_2\ f_c$ to be described on the screen). In that case one can work with low values of f_c even when f_i is lower than 200 c/s.

---

[4]) If it is desired to have two channels of high sensitivity a separate pre-amplifier, *e.g.* type GM 8002 or GM 4570, can be used for the second channel.

[5]) See, for instance, the second article listed in footnote 1, in particular fig. 3.

[6]) The said limits of f_i depend upon the frequency of the time-base. It is assumed that the latter is 1 to $^1/_4$ times f_i, thus that the oscillogram covers 1 to 4 cycles of the input voltage.

So far we have been assuming that both the input voltages are periodic. Obviously, in cases where one of the two (or both) occurs only once, f_c must be chosen sufficiently high for the switching to take place a number of times within the observation period (with such a frequency that the details to be investigated can be seen).

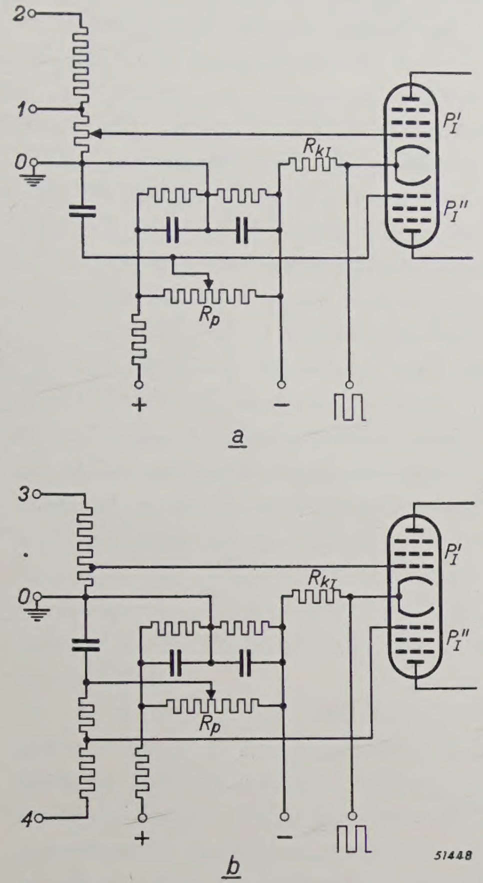

Fig. 12. The input circuit of each of the channels in the electronic switch GM 4580: *a*) for asymmetrical input voltage, *b*) for symmetrical input voltage. *0-1* input terminals for max. 50 V, *0-2* input terminals for max. 500 V, *3-4* input terminals for max. 2 × 500 V. R_p is a potentiometer by means of which the oscillograms can be moved up and down.

Table I gives a summary of the cases which may arise. To make it possible to select the optimum commutating frequency for each of these cases, with the new electronic switch this frequency has been made variable between wide limits, *viz.* from 2 c/s to 40 000 c/s.

This range is covered by varying the grid condensers in a multivibrator in a number of stages, combined with a continuous regulation of the grid resistance. In this way it is always possible to choose a value of f_c which is not exactly a multiple of the time-base frequency. The dots which go to make up the oscillograms when the commutation is rapid will then move along the curves to be described and thus traverse the whole of the oscillogram, including all details. The speed at which the dots move depends upon the value of f_c; by adjusting f_c so as to cause these dots to move rapidly one gets more the illusion of continuous curves.

Table I.

This indicates how the commutating frequency f_c can best be chosen in different cases. f_i = frequency of the input voltage in cycles per second, T = observation time in the case of non-periodic phenomena, expressed in seconds.

Input voltage	f_i	Recording	
		visual	photographic
		f_c/f_i	f_c/f_i
periodic	< abt. 200 abt. 200-1000 > abt. 1000	$\gg 1$ $\gg 1$ of $\ll 1$ $\ll 1$	$\gg 1$ or $\ll 1$ $\gg 1$ or $\ll 1$ $\ll 1$
non-periodic	—	f_cT	f_cT
		$\gg 1$	$\gg 1$

III) *Input circuits of the electronic switch*

The electronic switch GM 4580 is provided with symmetrical as well as asymmetrical inputs.

The asymmetrical input, illustrated in *fig. 12a* for one channel, is used when it is desired to oscillograph a voltage with respect to earth. According to the size of this voltage it is connected between the terminals *1* and *0* or between *2* and *0* (maximum values respectively 50 and 500 V). By means of a potentiometer R_p a variable and polar-reversible direct voltage can be taken up in the control grid circuit of P_I''. Thanks to the commutation this direct voltage corresponds to a rectangular alternating voltage on the output terminals. As a consequence the oscillogram of the corresponding

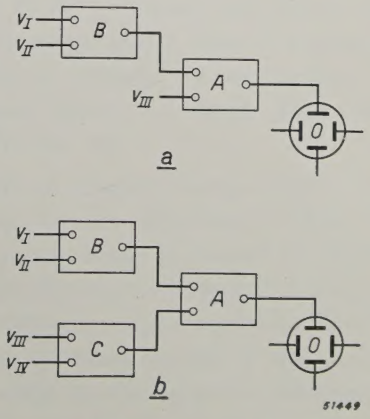

Fig. 13. Block diagram for the simultaneous recording of (*a*) three or (*b*) four oscillograms. *A*, *B*, *C* = electronic switches, *O* = oscillograph tube, $v_I \ldots v_{IV}$ = input voltages.

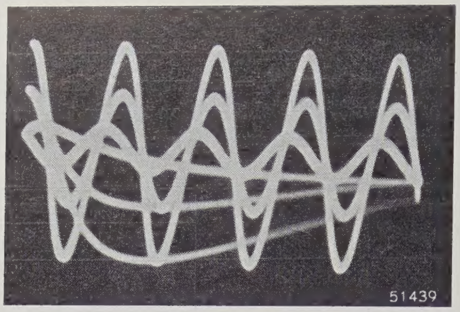

Fig. 14. Example of three oscillograms produced simultaneously.

input voltage moves upwards or downwards according to the polarity of the direct voltage. The potentiometers of the two channels are controlled with one knob and are coupled in such a way that when this knob is turned the two oscillograms move in opposite directions, so that they can easily be brought into a position that is most suitable for the observation.

The symmetrical input circuit is illustrated in fig. 12*b*. Here again we have the displacement device just described. We shall mention here two exceptional cases where the symmetrical input is useful on account of the symmetrical output of the preceding apparatus. In the first place such a case occurs when the oscillograph amplifier is used as pre-amplifier for one of the channels, as has been mentioned above. In the second place such a case is met with when it is desired to record more than two oscillograms together, by connecting electronic switches in cascade. The input of the electronic switch connected with the output of the preceding switch must then be symmetrical, because the said output is symmetrical.

This latter case is further illustrated in *figs. 13a* and *b*. According to these principles three oscillograms can be produced with the aid of two electronic switches, or four oscillograms with three such switches. An example is shown in *fig. 14*.

ABSTRACTS OF RECENT SCIENTIFIC PUBLICATIONS OF THE N.V. PHILIPS' GLOEILAMPENFABRIEKEN

Reprints of the majority of these papers can by obtained on application to the Administration of the Reseach Laboratory, Kastanjelaan, Eindhoven, Netherlands. Those papers of which no reprints are available in sufficient number are marked with an asterik.

1718: J. M. Stevels: The physical properties of glasses. V. A peculiar phenomenon in the vitreous system Na_2O-B_2O_3
VI. The relationship between the volume and the number of glass-forming ions in silicate glasses.
VII. The molecular refraction of glasses.
(J. Soc. Glass Technology, Trans **30**, 303-317, 1946 Aug.-Oct.).

V. The density-concentration curve of sodium borate glasses is determined and the S-shaped curve found is discussed. At a concentration of 4 per cent Na_2O a widening of the oxygen network is found which is not connected essentially with the sudden increase of the electric conductivity at this composition.
VI. It is shown that, at least in silicate glasses, there is no perceptible difference between the volumes of bridging and non-bridging oxygen ions. The volume of the interstices in the oxygen network is proportional to $R^{3/2}$ (R being the ratio of the number of oxygen ions to the number of glass-forming ions) as is deduced from a simple model of the glass structure. Using these two results the volume of a block of glass containing one gram-atom of oxygen is calculated as a function of R. The values obtained are identical, within the limits of errors, with those derived from a formula obtained previously.
VII. It is shown that the molecular refraction of abnormal glasses can be calculated in an additive way, with the aid of atomic (ionic) refractions, provided that distinction is made between bridging and non-bridging oxygen ions. This additivity is not expected for the normal glasses. These expectations are found to be realised for a large number of pure silicate glasses containing Na^+, K^+ and Ca^{++} ions only. The deviations between experimental and calculated molecular refractions for the abnormal glasses are less than 0.3 per cent. Glasses containing isolated oxygen tetrahedra are not examined.

1748: J. Hoekstra and C. P. Fritzius: De hechting van verf en vernis. (De Verfkroniek **20**, 195-198, 1947 Aug.) (The adhesion of paints and varnishes, in Dutch)

Paint adhesion may be defined as the energy necessary for lifting a unit surface of paint from its base. As it is practically impossible to measure this energy, a method is looked for in which a paint film is drawn from the base under specified conditions while the applied force is measured. The authors, choosing a shearing force rather than a force perpendicular to the film, describe a method in which the upper surface of two metal blocks with a metal strip between them is painted. After unscrewing, the strip is drawn off parallel with the paint layer (see also Philips Techn. Rev. **8**, 147-148, 1946).

1749: J. F. H. Custers: Diffusion of water into a polymer (J. Polymer Sci. **2**, 301-305. 1947)

In contradistinction to usual methods, the diffusion of water into a polymer has been investigated by starting from a disc of the material surrounded by water. In this way actual service conditions are often closely approached. Since a theoretical basis is desirable, equations are given for this type of diffusion and experiments with a wooden floor containing phenol-formaldehyde are described from which values for the permeation constant could be derived.

1750*: C. J. Bouwkamp and N. G. de Bruijn: The electrostatic field of a point charge inside a cylinder in connection with wave guide theory (J. Appl. Phys. **18**, 562-577, 1947 no. 6).

The field of a point charge inside a hollow, infinitely long, circular cylinder is studied. The case of an axial point charge is treated in detail. The surface density function is obtained as the solution of a Fourier type of integral equation. Then the potential caused by these charges is obtained. A second method works in the opposite direction. Here the potential is obtained as solution of a boundary value problem. A third method is based on the theory of Fourier-Bessel-Dini series. The potential is developed into discrete normal solutions of the potential equations in cylindrical coordinates. It is emphasized that the study of the potential problem can serve as a guide in questions of wave propagation in hollow circular cylinders. In this connection the third method is shown to be extremely useful. This is demonstrated in the case of acoustic waves inside a cylinder caused by a harmonically vibrating point source.

1751: N. Warmoltz: Variational principles in the theory of the cathode fall of a glow discharge (Physica **13**, 479, 1947 No. 8).

Attention is drawn to a recent remark of Seeliger (Phys. Z. **45**, 141, 1944) who criticizes Rogowski's theory of the cathode fall. One has to demand that a functoin, taking into account the formation (ionisation) and the transport of the ions as well, attains an extreme value for the real field ditribution. By following a procedure given by Seeliger it is possible to find an infinite number of these functions, but it seems difficult to select a function permitting a simple physical interpretation.

1752: C. J. Bouwkamp: A new method for computing the energy of interaction between two spheres under a general law of force (Physica **13**, 501-507, 1947 No. 8).

A new method is communicated, based on the theory of Bessel functions, for calculating the energy of interaction of two homogeneous spheres, on the assumption that $V(r)$ is the mutual potential energy of two unit point masses a distance r apart. Particularly, when $V(r)$ is proportional to the n^{th} power of $1/r$ an early result of Bradley is obtained. For integral values of n, subject to $1 < n < 8$ a limiting process leads to logarithmical terms.

1753: K. F. Niessen: On a cavity resonator of high quality for the fundamental frequency (Appl. Sci. Res. **B 1**, 18-34, 1947 No. 1)

The quality of a cavity resonator, the cross section of which is a parallelogram of a very special shape, is evaluated. It is shown that this cavity resonator may be used very well where a good quality is required without the possibility of lower frequencies occurring when the cavity is used as a part of a triode generator.

1754: M. J. Druyvesteyn: Experiments on the effect of low temperature on some plastic properties of metals (Appl. Sci. Res. **A 1**, 66-80, 1947, No. 1).

The yield value, breaking strength, elongation and hardness of a number of pure polycrystalline metals were measured at room temperature and at —183° C. The yield value was always higher at —183° C than at 20° C, the difference being relatively small (< 75 per cent) for the cubic face-centered and a number of hexagonal metals (e.g. Mg). The same difference is large for the body-centered metals and for Zn, Cd and Sn. The former metals have a larger elongation at lower temperatures; the latter, however, become more or less brittle at low temperatures. The breaking strength and the hardness generally increase with decreasing temperature.

1755*: J. A. Haringx: Over sterk samendrukbare schroefveren en rubberstaven en over hun toepassing bij trillingsvrije opstellingen (Dissertatie Delft 1947) (On highly compressible helical springs and rubber rods and on their application to vibration-free mountings; in Dutch).

The contents of this thesis will appear in full in Philips Res. Reports. A part of the subject has been treated in Philips Techn. Rev. **9**, 16 and 85, 1947, Nos 1 and 3.

1756: Balth. van der Pol: Wiskunde en radioproblemen (Simon Stevin **25**, Dec., 1947) (Mathematics and radio problems; in Dutch).

A lecture given before the Dutch "Mathematical Centre". The author treats the lack of mutual understanding sometimes found between technicians, physicists and mathematicians, each group speaking its own "language". The paper deals with the relation between Dirac's function and Stieltjes's integrals; Landau's O-symbol; Hurwitz's determinants characterising the stability of linear systems; the wave equation, diffraction round a sphere (propagation of radio-waves round the earth); continued fractions applied to filter circuits; non-linear differential equations as related to valve oscillators and, finally, modern electrical calculating machines.

1757: C. J. Bouwkamp: On spheroidal wave functions of order zero (J. Math. and Phys. **26**, 79-92, 1947 No. 2)

A survey is given of some of the results arrived at by the author in his dissertation (Groningen 1941; dealing with the diffraction of sound by a circular aperture and related problems): calculation of characteristic values and characteristic functions occurring in the separation of the wave equation in spheroidal coordinates; tables of numerical values.